Lifetime modelling of lead acid batteries

Bindner, H.; Cronin, T.; Lundsager, P.; Manwell, J.F.; Abdulwahid, U.; Baring-Gould, I.

Publication date:
2005

Document Version
Publisher's PDF, also known as Version of record

RISØ

Risø-R-1515(EN)

Lifetime Modelling of Lead Acid Batteries

Henrik Bindner, Tom Cronin, Per Lundsager,
James F. Manwell, Utama Abdulwahid, Ian Baring-Gould

Risø National Laboratory
Roskilde
Denmark
April 2005

Risø-R Report

Author: Henrik Bindner, Tom Cronin, Per Lundsager, James F. Manwell, Utama Abdulwahid, Ian Baring-Gould
Title: Lifetime Modelling of Lead Acid Batteries
Department: VEA, VES

Risø-R-1515
April 2005

Abstract:

The performance and lifetime of energy storage in batteries are an important part of many renewable based energy systems. Not only do batteries impact on the system performance but they are also a significant expenditure when considering the whole life cycle costs. Poor prediction of lifetime can, therefore, lead to uncertainty in the viability of the system in the long term.

This report details the work undertaken to investigate and develop two different battery life prediction methodologies with specific reference to their use in hybrid renewable energy systems. Alongside this, results from battery tests designed to exercise batteries in similar modes to those that they experience in hybrid systems have also been analysed. These have yielded battery specific parameters for use in the prediction software and the first results in the validation process of the software are also given.

This work has been part of the European Union Benchmarking research project (ENK6-CT-2001-80576), funded by the European Union, the United States and Australian governments together with other European states and other public and private financing bodies. The project has concentrated on lead acid batteries as this technology is the most commonly used. Through this work the project partner institutions have intended to provide useful tools to improve the design capabilities of organizations, private and public, in remote power systems.

ISSN 0106-2840
ISBN 87-550-3441-1

Contract no.:
ENK6-CT-2001-80576

Group's own reg. no.:
1115029-01

Sponsorship:

Cover :

Pages: 82
Tables: 10
References: 18

Risø National Laboratory
Information Service Department
P.O.Box 49
DK-4000 Roskilde
Denmark
Telephone +45 46774004
bibl@risoe.dk
Fax +45 46774013
www.risoe.dk

Contents

Preface

Power system implementers commonly agree that one of the key weak links in the long-term operation of renewable based rural energy systems is the system batteries. Batteries not only impact on the system operation and performance, but also can greatly affect the life cycle cost of a specific power system. Numerous hybrid power system performance and economic models, [1] that are currently in use provide an estimate of battery life based on a number of different mathematical calculations and assumptions. These life calculations are then used to develop cost of energy estimates for the power systems.

Unfortunately the varying methods currently used are quite diverse with many different assumptions and very little effort has gone into the validation of these methods. Additionally, most of the methods use calculation techniques based on information provided by manufacturers, usually under conditions that are not at all similar to the ones experienced by batteries in remote power systems.
Under the Benchmarking project work, two different battery life calculation methodologies have been investigated and further developed with the aim of improving the prediction of the life of batteries in hybrid power systems. One is based on a cycle counting approach similar to that used in structural fatigue analysis, the other is based on the application of a cross matrix, developed by the project for linking a number of stress factors with the recognised lead acid battery damage mechanisms. Both methodologies are combined with their own battery performance model in order to link the predicted battery life time with the actual use of the battery in terms of simulated or measured charge / discharge patterns.

The project combines the model development with experimental verification, using both specific lab tests of selected batteries as well as field test results collected in the project's systems test database. The reliable prediction of battery life in a given system is a precondition for providing a proper decision basis for system costs & performance, and the validation procedure established by the project is an essential part of this. The paper describes the first results of the battery model development effort as well as results from the initial model validation using standard battery performance testing for operating profiles considered representative of wind and PV powered remote power systems.

This work is part of the European Union Benchmarking research project (ENK6-CT-2001-80576), funded by the European Union, the United States and Australian governments together with other European states and other public and private financing bodies. It incorporates the combined experience of 12 internationally recognised research and development laboratories worldwide. Through this project the partner institutions intend to provide useful tools to improve the design capabilities of organizations, private and public, in remote power systems. This work also aims at engaging the manufacturers of components widely used in remote area power systems, to specify these components in terms that are relevant to the renewable energy systems industry.

1 Lifetime of batteries in RES applications

1.1 Application of batteries in RES systems

The nature of renewable energy sources makes it a challenge to integrate them in power systems. The two main characteristics of renewable energy sources that present challenges are their intermittency and their unpredictability. The impact of both these characteristics can be mitigated by the application of batteries in the system. The main issue in power systems with large amounts of renewable energy is to match economically the power production to the consumption. The intermittency of the renewable energy production means that storage or other types of production is needed in order to meet the demand. Power quality and stability also has to be ensured by the controllers of the system. The intermittency of renewable energy sources also has a significant impact on the layout and requirements for the controllers of the system.

Different types of renewable energy sources have very different characteristics both in terms fluctuations and in terms of power production technology. The major renewable energy sources investigated as part of the Benchmarking project are wind and solar electric power.

The solar input to a solar power plant naturally depends on the geographical placement of the plant. It will have a very significant component which depends on the time of day and year and another component that is dependent on the actual weather. It is this last component of the solar input that makes the input unpredictable, however, both of the above components of the solar input have an impact on the energy storage system. In Figure 1 solar irradiation is shown for a typical location in Denmark.

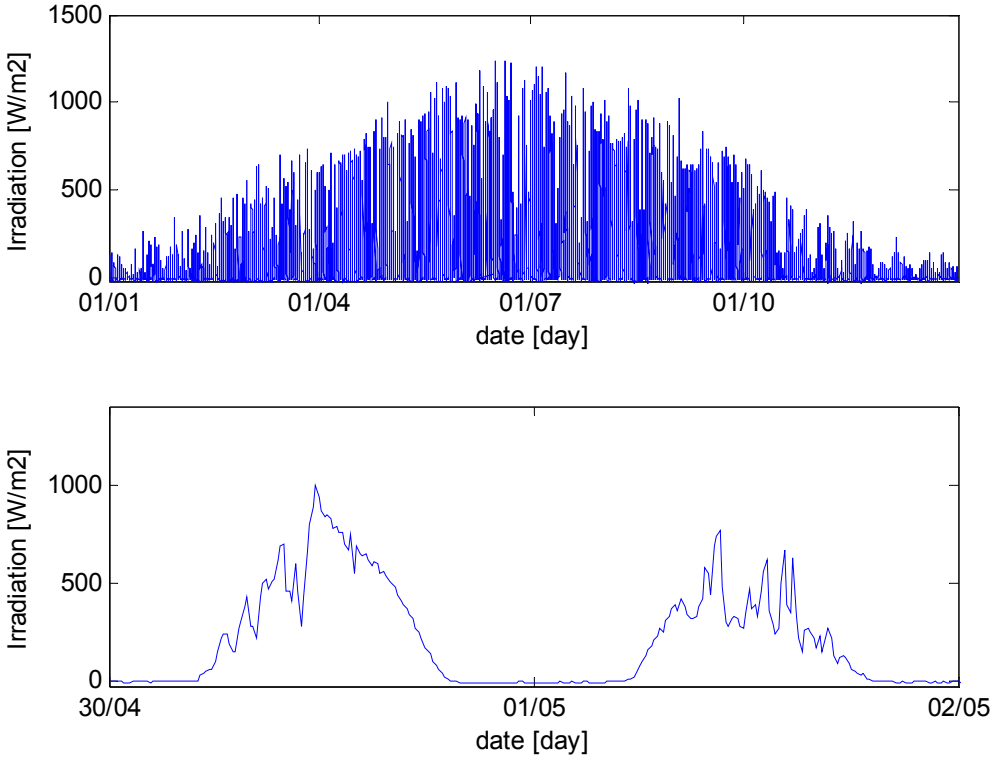

Figure 1 Solar Irradiation (5m a.s.l, horizontal) during 2004

It will often be the diurnal and seasonal variations that will determine the size of the battery because of requirements for the system to be autonomous. This will often result in a relatively large energy storage capacity compared to the load. Furthermore, the size of the PV array will be large enough so that it can fully charge the battery as part of the normal operation. The short-term fluctuations will, therefore, have a relatively small impact on the size of the battery storage.

The characteristics of the wind resource are in most places significantly different from the solar resource. Wind is much more fluctuating in nature and although there will be daily and seasonal variations the major part of the input will be stochastic and very difficult to predict. The stochastic part is usually referred to as the turbulence. Since the fluctuations are both faster and larger than for solar resources the operating conditions for an energy storage system will be significantly different. The structure of the wind resource is also very dependent on the site. Some sites have a very high turbulence intensity and some have a very steady wind even if they are close. To illustrate how a typical wind pattern looks, a year of data is presented in Figure 2 (10 minute average values).

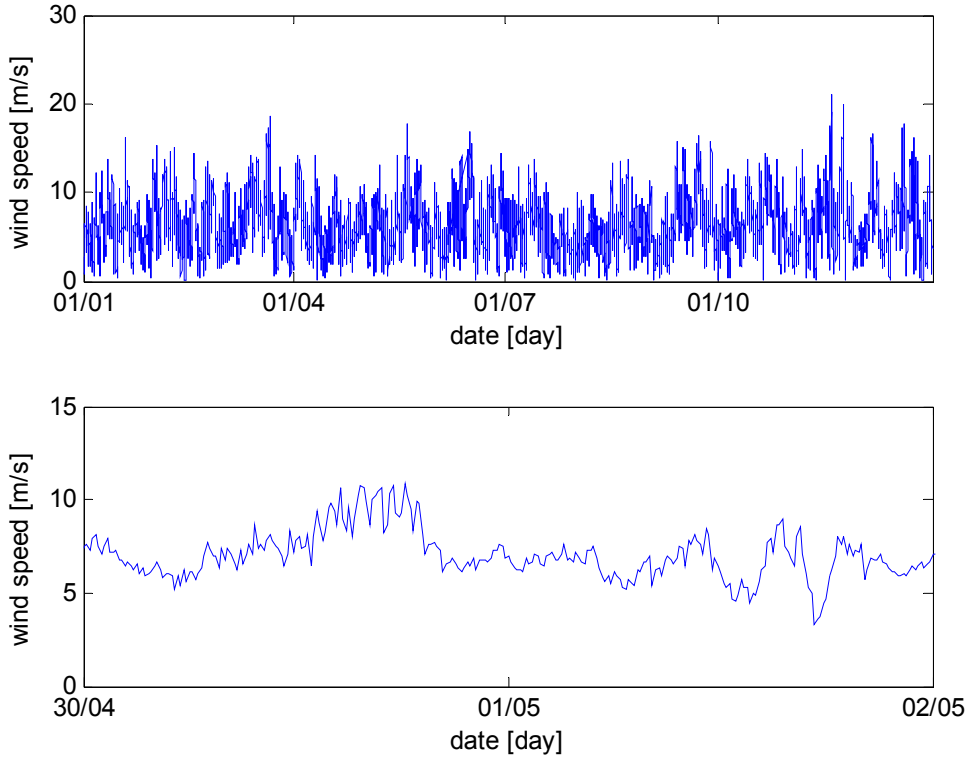

Figure 2 Wind speed measured at Risø (44m a.s.l, 10 minute average values) during 2004

Contrary to solar resources, a wind resource can have extended periods (days) with calm or very low winds (i.e. no wind energy production) and the short term fluctuations are on average much larger. In addition, the wind energy production is not proportional to the wind speed, but depends on the cube. These characteristics have a significant impact on how energy storage is integrated into the system.

Many layouts of power systems with renewable energy exist. They range from small solar home systems of 50-100W to large wind diesel systems of several mega-Watts.

Even within each type of system many variations exist especially regarding system controllers.

The primary objective for a solar home system (SHS) is to use solar energy to provide power for light and small residential appliances (TV and radio). This means that the battery included as part of the system will usually be charged during the day and discharged at night. The layout of a typical SHS is shown in Figure 3. It is the task of the charge controller, sometimes including a maximum power point tracker (MPPT), to maintain the efficiency of the system while keeping the batteries within their operating range i.e. by limiting voltages and currents.

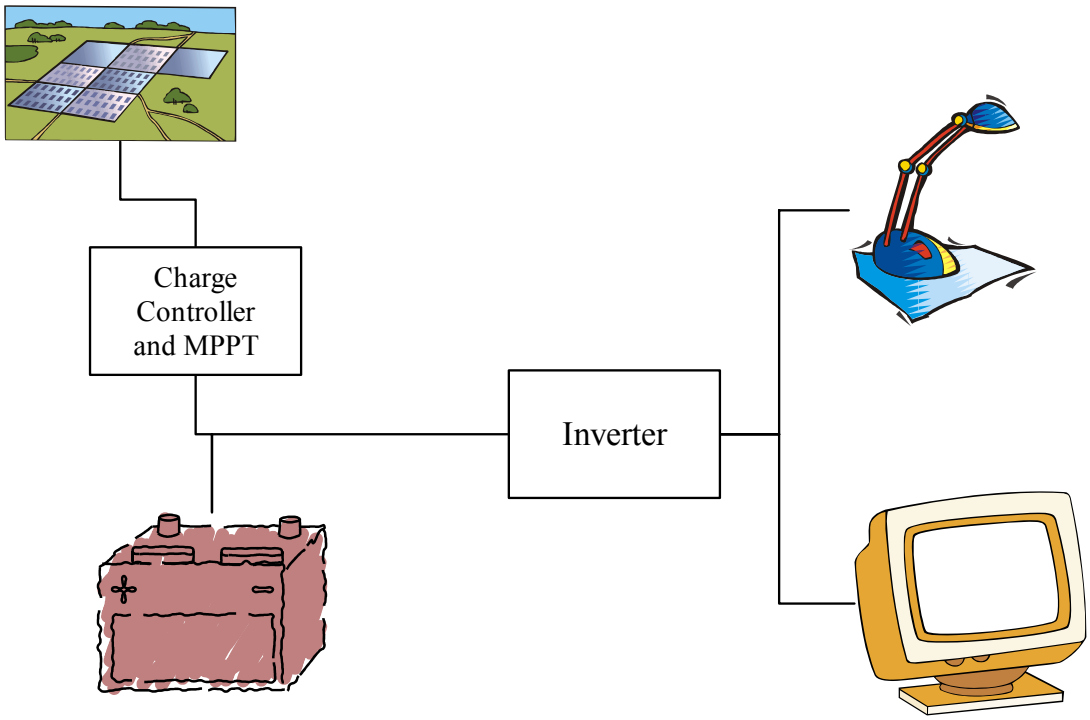

Figure 3 Solar home system with charge controller for battery control and inverter for AC generation

The corresponding type of system using a wind turbine is the small wind battery system or wind charger. Typically these systems will be larger than a SHS, ranging in size from 100W to 10kW. There will be a large difference in the applications for systems with such a power range. As for the SHS it is the task of the charge controller to ensure the operating conditions of the batteries are kept within limits. Since wind does not exhibit the same variations as solar irradiation, the operational conditions of the batteries will very different. The layout of such a system is similar to the SHS system except for the wind turbine replacing the PV modules.

For larger systems there will often be a requirement to supply power 24 hours a day. In such systems other types of generation will commonly be included, typically a diesel genset. This applies to systems with PV modules or with wind turbines, or a combination of the two. In such systems the battery capacity will often be smaller since the autonomy is guaranteed by the genset. The genset will also often be used as an active component in the battery management strategy, for instance to ensure the complete charging of the batteries. A typical system layout is shown in Figure 4. The system in the figure is AC-based and the genset is connected to the AC bus bar. Alternatives where the system is DC-based are also common. The output from the genset is then rectified and fed to the DC bus to supply charge to the battery bank.

The loads can be either DC loads connected to the DC bus bar or a central AC converter can be part of the system which then feeds the loads.

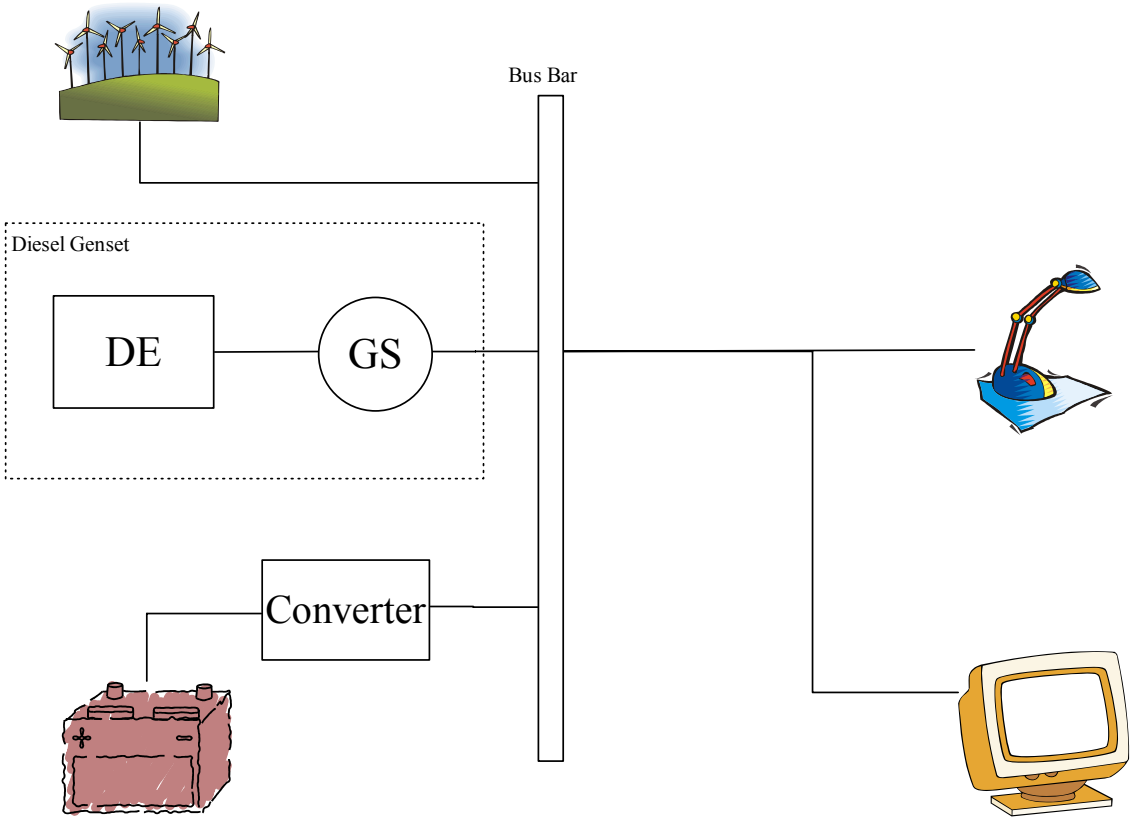

Figure 4 Simple wind diesel system with battery storage. Components are connected to a common AC bus bar

The nature of the wind resource leads to two ways of implementing batteries in wind based systems. Batteries are either chosen to provide small amounts of energy to ride through short lulls in wind power without the need to start a diesel engine or to provide large amount of energy storage that can give system autonomy even if there is no wind input for days. The first option will typically lead to battery sizes supplying 10-30 minutes of storage autonomy. The operating conditions of the power system with these two approaches will be very different for batteries in the two types of systems.

In systems with a small battery capacity the battery will experience large currents and frequent power reversals. In a system with a large storage capacity the relative currents in the battery system will be small and depending on how a back up diesel genset is being used, extended periods at partial state of charge are possible.

The design of the system usually depends on minimising the cost of energy given the constrains of the system in terms of technical performance and other requirements. Typically, system performance models such as Hybrid2, [2] , HOMER [3], IPSYS **Error! Reference source not found.**, will be used to assess the performance and provide input for the cost calculations. The major elements are the sizing of the components based on available renewable sources, the load, and the control of the system. Seen from the batteries' perspective the control strategy is very important and it includes several time scales from seconds to hours or even days.

To guide the system designer, categories of similar use of batteries in such systems have been defined as part of the Benchmarking project, [5], and these can be used to help select batteries that are particularly suited for a specific application or use profile.

1.2 Damage mechanisms and stress factors

The major components of a lead acid battery are the two electrodes, the electrolyte and the terminals. Many types of lead acid batteries exist and the construction of the batteries is adapted to specific battery applications. Some of the applications include car batteries (Starting, Lighting, Ignition (SLI)), truck or heavy duty and batteries developed for application in renewable power systems, especially PV systems.

The construction of the batteries differs in two ways: The construction of the electrodes and the electrolyte system.

The electrodes consist of a grid and the active material. The purpose of the grid is to distribute the current and provide mechanical support for the active material. Grids come in many shapes and material properties depending on the application of the battery. Plates in batteries for renewable energy systems and other deep cycle applications are primarily thick flat plates, tubular plates or spiral wound. Flat plate batteries are simple to manufacture. The tubular plate is more robust because the active material is contained in tubes, which will reduce shedding. Spiral wound plates are even more robust.

There are also many variations of electrolyte system: flooded, valve regulated (VRLA), absorbed glass mat (AGM) or gel. The two last types have the electrolyte immobilised by either a porous glass mat or through the addition of fumed silica gel. Immobilisation of the electrolyte reduces acid stratification (the condition where the concentration of the electrolyte is higher at the bottom than at the top).

The battery will be affected in different ways depending on the conditions under which it is operated. All types of lead acid batteries will suffer from the same damage mechanisms but to different degrees. In the Benchmarking project, a clear distinction has been made between the damage mechanisms of ageing processes, which are irreversible changes of the components of the battery (or the material composition of components), and stress factors which are characteristic features of the operating conditions of the battery and which alter the rate of action of the damage mechanisms. By themselves, stress factors do not change the components or materials of the battery, except for acid stratification which can be considered to be both a damage mechanism and a stress factor. The influence of a damage mechanism on the performance of a battery is a function of its design, selection of materials and manufacturing processes.

As part of the project the following major damage mechanisms have been identified, [5]. These are:

- Corrosion of positive grid.
- Hard/irreversible sulphation.
- Shedding.
- Water loss/drying out. (This is a damage mechanism for VRLA batteries. Water loss also occurs in flooded batteries but only causes damage if it is not replenished in time due to poor maintenance.)

- Active mass degradation.
- Electrolyte stratification. (This is a damage mechanism for VRLA batteries. For flooded batteries it can be considered to be a reversible effect which only causes irreversible damage if it is not removed in time.)

Corrosion of the positive grid has an impact on the internal resistance and available capacity. The internal resistance increases as the corrosion layer increases because of the reduced conductivity of the corroded material and due to the reduced cross section of the grid. The reduction in capacity results from the fact that as part of the grid corrodes, some of the active mass has reduced electrical connection to the terminals. There are several mechanisms that drive corrosion but the three main factors are battery voltage, acid concentration and temperature. The dependence on voltage is complex but in general high voltages increase the corrosion speed dramatically. As can be seen while looking at the other damage mechanisms, low voltages should also be avoided. Maintaining a battery at the float voltage results in the least corrosion. The major part of the research carried out on the impact of voltage on corrosion speed has been conducted by Lander, [6]. Increased acid concentration will also increase the corrosion speed. This is particularly important while considering stratification as the lower part of the electrode will experience higher acid concentrations when the battery is stratified. Elevated temperature also plays a key role is corrosion, the higher the temperature the faster the corrosion process.

As part of the fundamental chemical reaction of the battery, sulphate crystals are created at both electrodes when the battery is discharged. When the battery is charged the crystals dissolve and are converted to PbO_2 and Pb on the positive and negative electrode respectively. However, if the battery is not operated properly, such as left at a low state of charge for a long period of time, the sulphate crystals grow in size and large sulphate crystals are created. Since these large crystals do not dissolve easily when the battery is charged this leads to hard or irreversible sulphation. This in turn leads to a loss of capacity because the sulphated part of the active material is not longer active and the large sulphate crystals will leave part of the active material insulated from the terminal. Further, the sulphate crystals have a larger volume than PbO_2 (and Pb) which results in a higher mechanical stress on the electrodes.

Shedding is a process whereby some of the active material detaches from the electrodes and falls to the bottom of the battery, thus reducing the battery capacity. The process is influenced by sulphation because of the difference in volume of the sulphate crystals and the lead oxide on the positive electrode. Shedding can also be caused by overcharging the battery as gassing bubbles can detach active material from the electrodes.

Active mass degradation, also termed as softening of the electrodes, is primarily a change in the mechanical structure of the electrodes and active material. This leads to a decrease in porosity and surface area of the electrolyte and active material boundary. The decrease in surface area leads to a reduced capacity of the battery by concentrating the chemical reaction into less space and reducing the diffusion of the electrolyte. This degradation especially affects the positive electrode and cannot be restored by fully charging the battery because the degradation is a result of its exact discharge and charge history.

The last major ageing mechanism for the batteries is electrolyte stratification. In this process the acid content of the electrolyte stratifies, with the higher density electrolyte sinking to the bottom of the battery casing. Stratification leads to reduced battery capacity by concentrating the chemical reaction to specific parts of the electrodes and can increase corrosion at the top of the electrodes where the acid is weaker. Some disagree that this is a in fact a damage mechanism, or simply an accelerator for the other damage mechanisms already discussed. In flooded and VRLA batteries stratification can build up quickly, primarily dependent on the operating regime. Stratification can however be removed by overcharging the battery, creating gas bubbles which stir and mix the electrolyte. For batteries where the electrolyte is immobilised, stratification will usually not build up. This is the case for AGM and gel batteries.

Certain features of the operating conditions have a particularly strong impact on the damage mechanisms. These features are termed stress factors. Stress factors are quantities that are derived from the voltage, current and temperature history of the battery operation. The project has identified the major stress factors and their impact on the damage mechanisms. The major identified stress factors are:

- Discharge rate
- Time at low state of charge
- Ah throughput
- Charge factor
- Time between full charge
- Partial cycling
- Temperature

The definitions of the stress factors are in [5].

Table 1 shows the impact of the stress factors on the damage mechanisms found including the relative importance of the impact.

Table 1 Stress factors and their impact on damage mechanisms (light blue: strong impact; yellow: medium impact; green: little impact)

	Corrosion of the positive grid	hard/ irreversible sulfation	shedding	water loss / drying out	AM degradation	electrolyte stratification
discharge rate	Indirect through positive electrode potential	higher discharge rate creates smaller AM sulphate crystals and leads to inhomogeneous current distribution causes inh. SOC on the electrode	probably increased shedding; outer AM fraction cycles at higher DOD level cycling [pasted plates]	none	increases inner resistance due to AOS-model (agglomerate of sphere)	Higher discharge rate reduces electrolyte stratification. On the other hand less homogeneous current distribution plays negative role.
time at low states of charge	Indirect through low acid concentration and low potentials	A strong positive correlation: longer time at a low SOC accelerates hard/irreversible sulphation.	no direct impact	none	None	Indirect effect Longer time leads to higher sulphation and thus influences the stratification.
Ah throughput	no impact	no direct impact	impact through mechanical stress	no direct impact	loss of active material structure, larger crystals	A strong positive correlation: Higher Ah throughput leads to higher stratification
charge factor	a strong indirect impact because a high charge factor and an extensive charge is associated with a high charging voltages (high electrodes' polarisation)	negative correlation, impact through regimes with high charge factors which reduces the risk of sulphation	strong impact through gassing	strong impact	no direct impact	A strong positive correlation: Higher charge factor leads to lower stratification
Time between full charge	Strong negative correlation: shorter time increases corrosion.	Strong positive correlation: Frequent full recharge decreases hard/irreversible sulphation.	A negative influence, increasing with decreasing time.	A negative influence, increasing with decreasing time	no direct impact	A strong positive correlation: Higher Ah throughput leads to higher stratification
Partial cycling	An impact through potential variations (depends on frequency, SOC level, ..)	A positive impact. Higher Ah throughput at lower SOC increases sulphation. Partial cycling (f>1Hz) increases size of lead-sulfate crystals.	no direct impact However when the PC is of the minimal value, then the Ah throughput runs at very high SOC level and always to full recharge. It is also reflected by the "time between full recharge"	no direct impact However when the PC is of the minimal value, then the Ah throughput runs at very high SOC level and always to full recharge. It is also reflected by the "time between full recharge"	no direct impact However certain partial cycling may cause a preferential discharge and faster AM degradation in certain AM fraction.	Higher partial cycling at lower SOC leads to higher stratification.
Temperature	Strong impact, positive correlation	On one hand high temperature helps to better fully recharge (more sulfate can be recharged). On the other hand high temp. leads to more hard sulfate build up at a low SOC.	no direct impact	increasing with increasing temperature	low impact high temperature degrades neg. electrode expanders	no direct impact.

1.3 Benchmarking context

The use of batteries in RES has been investigated as part of the Benchmarking project, [7]. Data from many power systems were analyzed and similar use profiles of the batteries have been identified. This has lead to a grouping of systems in six different categories, depending the operating regime of the batteries,[5].

In order to provide recommendations on which battery type(s) to use for a particular system or application a standard method of analysing the system has been developed, a tool called THESA, to produce input for a decision support tool, called RESDAS, that provides the recommendations. The recommendations can then be used as part of the input into a system performance model that estimates the technical and economic performance of the power system. The results of the simulations can then be fed back into the THESA package for further analysis and after that into RESDAS to see if the system still falls into the same category. However, because the battery operation may change due to the use of a different battery, the process may lead to modifications of the recommendations, suggesting a new battery type. The tools, THESA and RESDAS, can also be used as a basis for choosing different system layouts and components that may be relevant for the site under investigation.

Power system performance models play a very important role in the assessment of both the technical and economic performance of systems. It is a key issue to have the ability for the comparison of different design options objectively. It is therefore necessary that the system models are able to model accurately the systems under investigation, including the control of the system and the battery storage. Additionally, to be useful in determining the appropriate battery technology the output of the system performance models should provide information required by the THESA tool, primarily battery voltage, current, SOC and temperature. It is essential that the controls of the system are modelled as closely as possible to the real system so that the output from the simulation models can accurately assess the lifetime of the batteries. For systems with wind input, short time steps, in some cases down to 5 seconds, are necessary for the correct simulation of the operating regime of the batteries.

2 Battery lifetime modelling

2.1 Battery modelling in general

Modelling of batteries is a very important aspect of hybrid power system simulation because the uncertainty associated with the expected lifetime of the batteries makes the estimates of cost of energy of the projects very uncertain. Since the life cycle cost of the batteries is one of the significant power system expenses it is a major source of uncertainty for potential power system investors.

Most battery models focus on three different characteristics. The first and most commonly used model is often termed a performance or a charge model and focuses on modelling the state of charge of the battery, which is the single most important quantity in system assessments. The second type of model is the voltage model, which is employed to model the terminal voltage so that it can be used in more detailed modelling of the battery management system and the more detailed calculation of the losses in the battery. The third type of model is the lifetime model used for assessing the impact of a particular operating scheme on the expected lifetime of the battery.

These different models can be independent of each other or they can be integrated and interdependent in an attempt to model the whole battery system.

If the lifetime model is independent of the performance and voltage models it can be used for post processing of output from other system models. The integrated models have the advantage that the degradation of the battery performance is modelled as the battery is being used. Many combinations of these three models are currently in use.

Since this report focuses on battery life modelling this is described in depth in the next section. Further information on modelling the capacity and voltage of batteries is discussed in the particular sections of this report that address specific models or in works by Nickoletatos & Tselepis, 2004 and Manwell & McGowan, 1993, 1994, [12], [16], [17].

2.2 Lifetime models

Many types of lifetime models for lead acid batteries exist. The main general types are:

- Post-processing models
- Performance degradation models

2.2.1 Post-processing models

The post-processing models are pure lifetime models in that they do not contain a performance model. They can therefore be used to analyse measured data from real systems. The performance degradation models combine a performance model with a lifetime model where the performance model is being updated during the simulation

so that the performance of the battery degrades as time goes by depending on the utilisation pattern of the battery.

There are many different methods for calculating the lifetime consumption. They will usually involve either directly or indirectly the above mentioned stress factors. They can either be used on their own in various combinations in order to include several phenomena.

The methods include

- Ah-throughput counting
- Cycle counting

The Ah-throughput model simply counts the amount of charge through the battery. The end-of-life criterion is based on the datasheet value for nominal charge throughput. Ah-throughput models can be extended to include weighting factors on the current depending on a number of factors such as the state of charge. Simple Ah-throughput models primarily focus on the Ah throughput stress factor and do not directly consider the other stress factors previously discussed. However, with the addition of specific weighting factors some of the stress factors can be accounted for.

The cycle-counting model mostly concentrates on current and state of charge of the battery. Here the assumption is that the amplitude of a charge cycle determines the fraction of lifetime that is consumed. This means that even though the charge throughput is the same the lifetime consumption can be different depending on whether the battery is cycled at large amplitudes or small SOC amplitudes. This method can also be modified to include more factors such as at what state of charge the cycle occurs. The end-of-life criterion is the number of charge and discharge cycles as specified in datasheets provided by most manufacturers. Since the number of cycles until end-of-life often varies based on the depth of discharge, the life consumption needs to be calculated by appropriate summation of the individual cycles.

2.2.2 Performance degradation models

The second type of general model is a performance degradation model, which follows more closely what the batteries are actually experiencing. In real batteries the useful life is generally expressed as the loss of the battery's ability to provide a specific amount of its original nominal capacity, usually 80%. So, for example, if a battery that has been operating for years is only able to supply 75% of its nominal capacity during a capacity test, the battery is considered dead. One of the important distinctions of this modelling method is that it generally combines all three of the battery models, voltage, capacity and life, by changing the parameters that model voltage and capacity until the battery can no longer meet the life requirement. This integrated approach therefore intrinsically accounts for the change in battery performance as it ages, something that the post-processing models cannot do. When using the performance degradation model a number of methods can be used to keep track of the reduction in performance of the battery capacity and when this capacity is reduced below a specified threshold the battery is also considered dead. There are two main methods to assess battery performance; the first uses an equivalent circuit model while the second attempts to model the physical properties of the electrolyte and electrodes.

The equivalent circuit lifetime model modifies the values of the parameters of the equivalent circuit voltage and capacity depending on the operating conditions of the battery. The updating methods of the equivalent circuit parameters can be based on current and charge using the same methods as in the Ah-throughput models or they can be based on the voltage and temperature or combinations of the different lifetime methods. The physical properties model describes the changes in the structure of the electrodes, leading to changes in how the electrolyte diffuses and thus its capacity and voltage characteristics.

The different types of lifetime models differ in complexity as well as in their requirements for data. The two first types require data for the battery that is generally available from the battery manufacture whereas the others, especially the physical properties models, require data that can only be acquired by having access to how the battery is constructed in very fine detail.

2.3 Types of models investigated in the project

Two existing lifetime models have been investigated and extended as part of this project. They are a rainflow counting model developed by UMASS as part of the battery model in the simulation package Hybrid2, [2], and an equivalent circuit model initially developed by FhG ISE as part of a PV system model, [8]. A third model, an Amp-hour counting model as is used in the simulation package HOMER, [3], was also evaluated although efforts were not made to improve the model's accuracy.

3 Lifetime and parameter tests of batteries

A very essential part of the battery lifetime modelling activity has been a model verification exercise to determine the accuracy of the different life prediction methods discussed for different operating regimes of the battery. This process was conducted in two testing stages, the first to determine the parameters required to model the specific battery and the second as a comparison between the models and long term lifetime tests of batteries using purpose developed testing profiles derived from experience with wind and PV systems.

Because the Benchmarking project was looking at lead acid batteries for different applications it was determined to complete testing on the two most common types of batteries used in renewable energy systems. The following two batteries were selected due to their common use and availability and access to the poles of individual cells.

- BAE OPzS 50: 12v 50Ah VLA tubular positive and grid negative electrode.
- BAE OGi 50: 12v 54Ah VLA round-grid positive and flat plate negative electrode.

3.1 Parameter tests

3.1.1 The need for specific parameter tests

Most battery models use the Shepherd equation for determining the output voltage of a cell, [9], [13]. This equation describes the variation of voltage with state of charge and current throughput. The parameters in the equation can be related to physical or chemical attributes of the battery and are thus different for each type of battery.

With four parameters for each charging and discharging equation, the requirement is, ideally, charge and discharge tests at four different constant currents. Unfortunately, these are generally not available from manufacturers or their data sheets. It was, therefore, decided that the Benchmarking project would carry out its own specific parameter tests for each of the two batteries.

3.1.2 Parameter test requirements

There are four points of particular interest during each discharge/charge sequence:

1. Point defined as full state of charge
2. Point where the voltage crosses the lower voltage limit during discharge.
3. Point defined as full depth of discharge.
4. Point where the voltage crosses the upper voltage limit during charge.

In order for the parameter tests to be useful for calculating the battery parameters these points, and those in between, need to be defined by voltage, current and state of charge.

The impact of battery temperature is not an integrated parameter in any of the models and thus measurements at different temperatures were not carried out as part of the test exercise. The temperature for these tests was kept constant using a fluid bed and if temperature flexibility were to be added to the models, additional testing could be undertaken to determine characteristic parameters for this as well.

3.1.3 Problems and Considerations

Defining and then conducting the tests to determine the above listed points for each current sequence were the main concerns in designing a useful battery parameter test.

The full state of charge is fairly well defined as the point at which the battery accepts no more charge after a standard charge with an I_{40} current for two hours. The voltage is also stable at this point.

The point at which the voltage crosses the lower voltage limit is also easy to define and achieve. A voltage of 1.8V per cell was chosen as a commonly accepted "empty battery" point.

More complicated however was how to describe a method to define the fully discharged criteria so that each charge test could start from the same state of charge. Stopping the discharge at 1.8V results in a voltage "bounce back" or recovery, the severity of which depends on the rate of discharge previously carried out. Therefore, should the battery be further discharged to reach a point with little or no recovery? As more capacity is obtained the lower the discharge current, it was argued that the battery should be discharged at a very low rate to achieve an absolute "empty" state. However, even then the ability to achieve a repeatable absolute empty battery was questionable. The alternative is to recharge the battery fully after every discharge test and then perform a standard discharge to 1.8V at a specified rate so that even though the recovery effect is experienced and somewhat unquantified a more constant state of charge is achieved every time in preparation for the charge test.

The point at which the voltage crosses the upper limit is, once again, easily defined and a limit of 2.4V per cell was chosen. A standard discharge and charge would then be performed to achieve a consistently full battery again.

It was decided that the nominal capacity of the battery would be used as a reference as opposed to the initial capacity of the particular test battery1. This, of course, meant that it was likely that negative states of charge would be encountered as the battery capacity is generally larger than its nominal or nameplate capacity. Negative states of charge are also encountered since the nominal capacity is defined by an I_{10} discharge rate and a battery subject to lower discharge rates producing more capacity.

In order to achieve a good spread of charge/discharge curves over a good operating range the following rates were chosen: I_5, I_{10}, I_{20} and I_{50}.

1 In this report quantities that are referenced to the initial capacity are maked with a *****. For example, I_{10}* is the current that fully discharges a battery from its initial capacity, C_{10}*, in 10 hours. The nominal, or manufacturer's rated, capacity is denoted C_{10}, and the corresponding 10-hour discharge current is I_{10}.

3.1.4 Parameter Test Profile

An example of the parameter test procedure is shown in Figure 5 and described below:

Parameter test:

1) Charge the battery with standard charge (IUIa as below, with the highest current rating possible).
2) Discharge the battery with the test current 1 (1.8V/cell). Rest period of 2 hours.
3) Charge and discharge the battery with the standard cycle as under 1.
4) Charge the battery with the test current 1 (2.4 V/cell). Rest period of 2 hours.
5) Discharge and charge the battery with standard cycle.
6) Discharge the battery with the test current 2.

….. and so on.

The standard IUIa charge:

I phase: constant current I_5 or higher (40 A/100 Ah) to 2.4V/cell,
U phase: 2.4V/cell limited by current $<I_{40}$ (2.5A/100Ah)
Ia phase: constant current I_{40} limited by 2 hours time (the voltage ought to be very close to a stable value and should definitely not increase further quickly) and safety voltage U=2.7V/cell (and or (by a charge factor if specified by manufacturer)

Rest time after the charge: 1 hour

The standard discharge:

Constant current I_{10} to 1.7V/cell
Rest time after the discharge: 1 hour

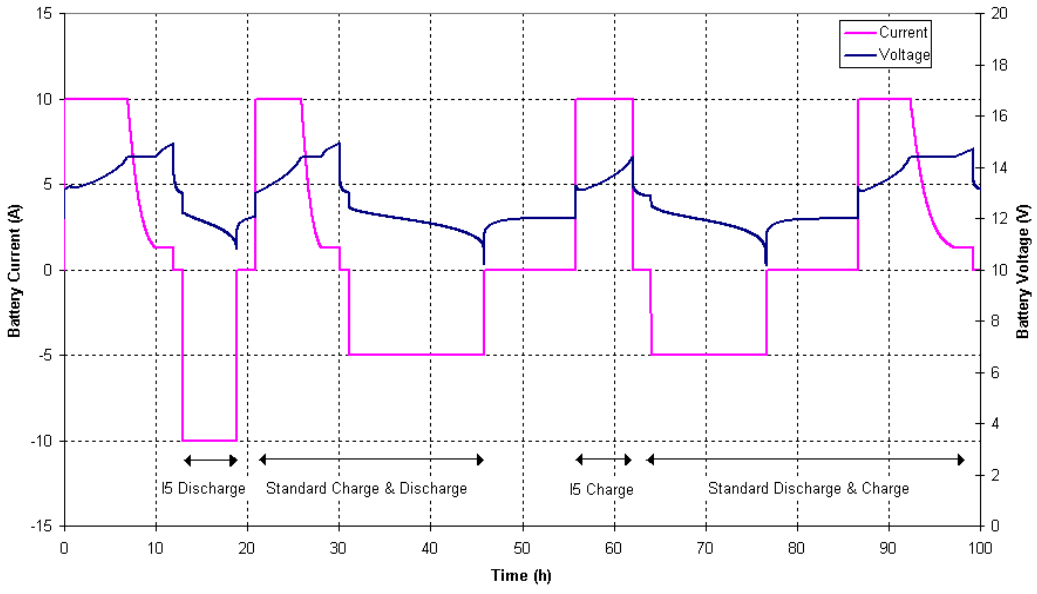

Figure 5 Example of I_5 Parameter Test Profile (OPz Battery)

From Figure 5 it is seen that the two hour constant charge current period is not long enough to reach a full charge since the voltage increasing. However, it is considered that this will introduce only a small and negligible error.

3.2 Wind and PV test profiles for lifetime assessment

Within the Benchmarking project the two types of battery chosen are being subjected to two types of use profile. Each profile developed was proposed to be somewhat characteristic of the current profile a battery would typically be subjected to when used in a renewable energy system: one photovoltaic system ("PV profile") and one wind power system ("Wind profile"). In order to track the decline of battery performance periodic capacity tests were performed.

Through the benchmarking project it became clear that a new series of life time prediction tests were required. When looking at power systems incorporating wind this need was evident as prior to the project no battery use profiles with wind as an input had been developed or tested. The variable nature of wind results in higher charge rates than are normally expected in PV systems and thus result in a unique battery use profile. More research has gone into the development of profiles for PV systems; however the profiles that are available have focused on either repeating quite general charge and discharge cycles, more typical for Solar Home Systems, or were designed to target specific damage mechanisms. Very few profiles had been developed that provide behaviour that would be typical of a hybrid PV power system. More information on the available testing profiles can be found in O. Bach et. al. 2002 and 2003 [10] & [11].

3.2.1 Renewable energy system profiles

The profiles shown in Figure 6 were used to represent a typical current profile required of a battery in a PV and in a wind system. The actual current used in the test is calculated as a multiple of the I10 current with reference to the initial capacity value and not the nominal value to ensure comparable conditions. The values shown here are for the OPz battery with an initial capacity (C_{10}*) of 70Ah.

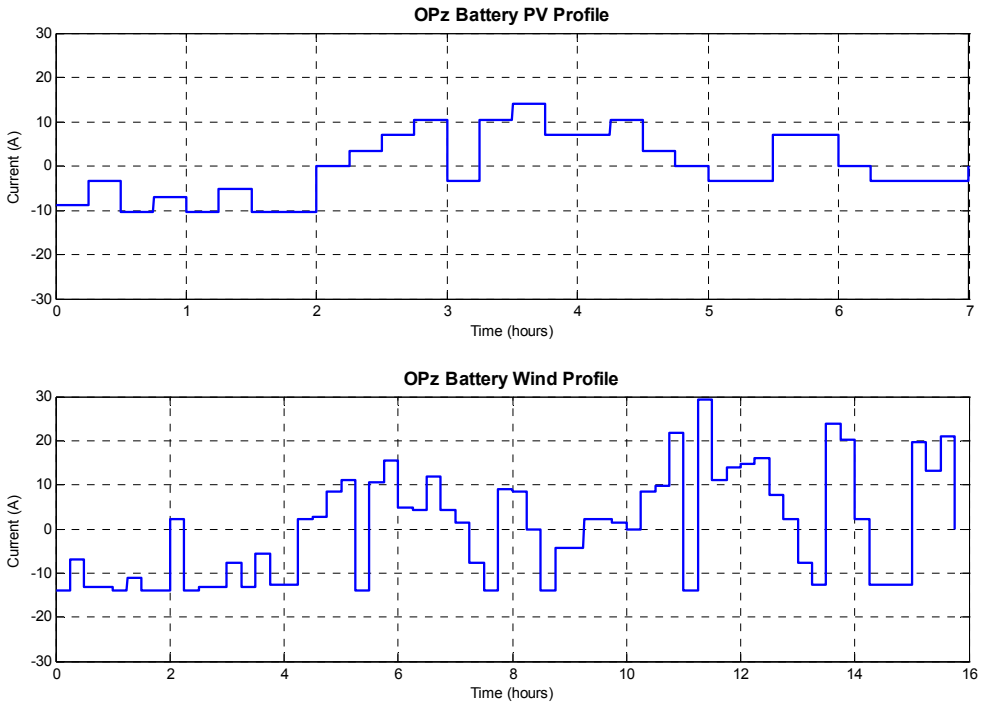

Figure 6 PV and Wind Profile Examples

Key figures for each test profiles are provided in Table 2, [12]. It is seen from the table and the figure that the magnitudes of the current in the wind profile are higher than in the PV profile. This reflects the experience with systems including wind compared to PV. It can be expected from the profiles that the batteries tested with wind profile will degrade faster than those tested with the PV profile due to the higher currents and higher rates of change of the current (for the same Ah throughput).

Table 2 Key figures for the test profiles (the currents and capacities are referenced to the initial capacity C_{10})*

Item	**PV**	**wind**
Duration [h]	7	15.75
I_{max} [I_{10}*]	2	4.2
I_{min} [I_{10}*]	-1.5	-2
SOC range [% of C_{10}*]	27.5	73.25
Ah throughput [C_{10}*]	0.3125	1.155

3.2.2 Battery test procedures

The batteries were first subjected to five I_{10} discharge / I_{10} charge cycles to condition the batteries and to try to obtain the real full capacity of the batteries. A capacity test then followed and this was designated to be the initial capacity.

The tests then consisted of blocks of repeated renewable energy system profile cycles interspersed with capacity tests.

The PV blocks were as follows:

1. Discharge at I_{10}* for two hours (to reach 80% SOC)
2. Series of 35 PV profile cycles.
3. Discharge at I_{10}* for three hours (to reach 50% SOC)
4. Series of 35 PV profile cycles.
5. Charge at I_{10}* for three hours (to reach 80% SOC)
6. Series of 35 PV profile cycles.

The voltage limits were 1.8V and 2.45V per cell.

The wind blocks were as follows:

1. Discharge at I_{10}* for one hour (to reach 90% SOC)
2. Series of 50 wind profile cycles.

The voltage limits were 1.75V and 2.45V per cell.

The capacity tests consisted of three types of capacity measurement.

1. Residual capacity. This was designed to define the capacity left in the battery at the end of that particular block of profiles.
2. “Solar” capacity measurement. This estimates the capacity of the battery if it were to receive a “full” charge typically experienced by a battery in a photovoltaic system.

3. Full C_{10} capacity. This gives the true full capacity of the battery after a IUIa charge where all active material is converted and there is a complete removal of stratification.

At the beginning and end of the whole test procedure a C_{100} capacity test was carried out.

The tests on the batteries have been carried out at three laboratories: CRES, JRC ISPRA and GENEC. For full details of the tests please refer to the Benchmarking report deliverable of WP4.2, [12].

4 Ah Throughput models

4.1 Model description

An Ah-throughput model assumes that there is a fixed amount of energy that can be cycled through a battery before it requires replacement, regardless of the depth of the individual cycles or any other parameters specific to the way the energy is drawn in or out of the battery. In most cases the estimated throughput is derived from the depth of discharge vs. cycles to failure curve provided by the manufacture, as shown in Figure 7, and Table 3.

This process is based on the observation that for many lead acid batteries, if the cycles to failure at each depth of discharge is multiplied by the energy returned from that discharge, the resulting curve can be assumed to be flat, shown as the calculated throughput on Figure 7.

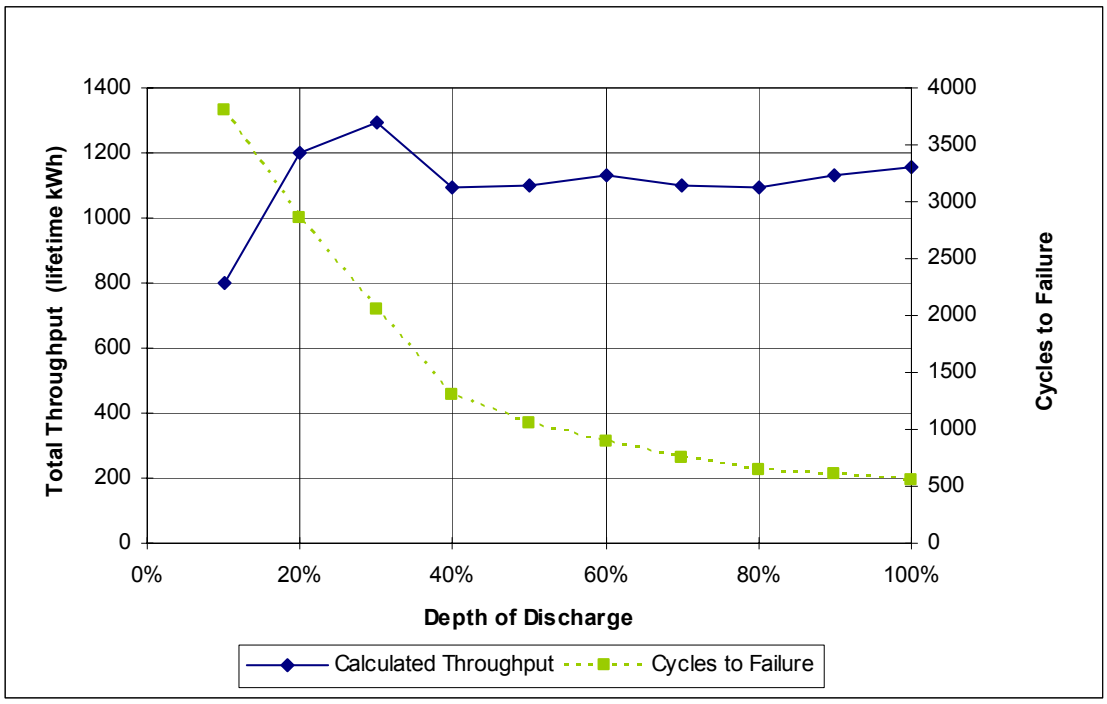

Figure 7 Cycles to Failure and Total Throughput for a Flooded Flat Plate Battery based on data supplied be the manufacturer

The expected throughput is defined by the following equation:

$$Throughput = Average\left\{ \left(E_{Nom}\, DoD_i \right) * C_{F,i} \right\}_Y^X$$

E_{Nom} = Nominal battery capacity

DoD_i = Specific depth of discharge being considered

$C_{F,i}$ = Cycles to failure to the specific depth of discharge

Where *i* represents each depth of discharge measurement provided by the manufacture, 10 values in the case of Table 3, and X to Y the

range over which the measurements are taken, 10% to 100% DOD in this case.

In most cases the lifetime throughput value is calculated based on an average of the throughput for each depth of discharge. This average can be taken for all depth of discharge cases or over the typical depth of discharge range that is expected to be used, such as between 0 and 60 %, represented by X and Y in the above equation. The result is one number that indicates the total number of Amp hours or Watt-hours that can pass through the battery before it is expected to fail.

To determine the expected life of a battery in a power system, the battery model then sums the Amp hours or Watt hours that pass into or out of the battery and when this value reaches the total throughput calculated for the battery, the battery life is considered used up.

Table 3 Example potential throughput life calculation for a 2.1 kWh battery with discharges from full state of charge to various depth of discharges.

Depth of Discharge	# of Cycles to Failure	Calculated Throughput (kWh)
10%	3800	798
20%	2850	1197
30%	2050	1292
40%	1300	1092
50%	1050	1103
60%	900	1134
70%	750	1103
80%	650	1092
90%	600	1134
100%	550	1155

Battery manufacturers create their cycles to failure data using specific testing requirements, usually at a constant temperature of 25^{o} C with the condition that when the battery capacity diminishes to 80% of its nominal capacity it is considered dead. As with the cycle counting method, the throughput method relies on battery manufacturer's data to calculate life and cannot easily assess battery degradation with use or battery operation for systems where the battery has dropped below the useful life specified by the manufacturer.

One of the key aspects of the throughput model is its simplicity, especially from a modelling perspective. Throughput calculations can use either Amp hours or Watt-hours, allowing more modelling flexibility.

A modified throughput model is used with the HOMER software, developed by the National Renewable Energy Laboratory, [3], to model distributed power systems. In the HOMER software a float life value is also included to specify the maximum life of a battery, regardless of throughput. The software also allows the user to select a minimum state of charge. This becomes the minimum of the range over which HOMER averages the lifetime throughput values. The HOMER model uses a simplified version of the Kinetic Battery Model, as described in section 6, to model battery capacity but does not model battery voltage. At this point in time the battery model in the HOMER software cannot be run independently nor can the output of the model be entered into the THESA model to assess proper battery selection as discussed in section 1.3.

4.2 Comparison with measurements/test results for validation

Cycle to failure data was obtained from the manufacturer for the OPzS battery which, when combined with the cycle to failure tests for the individual batteries, as described in section 3.2, allowed assessment of the total Amp hour throughput method. Based on the calculation method described above the battery was expected to provide 51,700 Ah of storage throughput assuming a complete battery discharge range of 10% to 100% DOD, or 44,450 Ah using a typical depth of discharge range of 0 to 60 % DOD.

Specific cycles to failure data could not be obtained from the manufacture for the OGi battery so an estimated cycles to failure curve was determine based on data from other flat plate batteries. Using this analysis it was determined that the OGi battery would be expected to achieve a theoretical throughput of around 15,500 Ah when covering the complete battery discharge range of 10% to 100% DOD or 13,300 Ah using a typical depth of discharge range of 0 to 60 % DOD. However, this life prediction data is based heavily on other batteries of similar type and thus should be considered suspect until further tests can be performed.

To compare the results of the throughput estimation method the total throughput to failure of each tested battery was summed for the different renewable profiles. The results are shown in Table 4. To allow a clearer way to look at the impact of the modelling error, the expected time error (in years) associated with the installation of a battery that would be expected to last 6 years is also provided.

Table 4 Comparison of Experiments and Throughput Method

	Calculated lifetime throughput (Amp hours)	Throughput to failure based on test data (Amp hours)	Error in method (%)	Actual Battery life based on testing (Years)	Modelled battery life (Years)	Difference over a typical six year battery life (years)
OGi Wind profile	13,300*	18,701	16.7	0.477	0.556	1.00
OPzS Wind profile	44,450	31,210	-17.5	0.882	0.728	1.05
OGi PV profile	13,300*	16,232	9.8	0.655	0.719	0.60
OPzS PV profile	44,450	Life cycle tests not completed	**	**	**	**

** Value based on estimated cycle to failure data*
*** Data is not available. Tests ongoing*

It should be noted that the experimental life cycle throughput used in these calculations are for a single battery and therefore are suspect due to the variances usually found in different batteries. Under the framework of the Benchmarking Project more batteries are being tested but these tests have not been completed at the time this document is being written. Once more data sets are available this analysis should be expanded.

The throughput method provides a reasonable estimate of battery life although over the life of a rural energy project, typically 20 years, the modelling error may result in one battery bank replacement. It should be noted that there is a significant difference in the throughput based on the different testing regimes used. In the wind case the battery endured higher throughput before failure, possibly due to the higher currents. Of additional interest is the difference in the results based on battery type. The throughput method underestimated battery life in the case of the flat plate OGi battery but overestimated the battery life for the tubular OPzS battery. More testing will have to be conducted to determine if this is an isolated case, but if found to be true would indicate that battery type correction factors would have to be determined to make up for this difference in life prediction.

4.3 Recommendations on potential improvements

Options would include the addition of scale factors that could be added to account for the lower relative damage caused by various conditions, such as the higher throughput associated with higher current applications. More simply a scale factor could be added to the throughput for specific battery types. Unfortunately, as stated previously, these approaches are complicated in the absence of a method to determine what these scale factors would be without extensive testing of the batteries being considered or at least more testing of different battery types. Improvements were not made to the general throughput method or the HOMER simulation software, one of the prime analysis tools that use this approach.

5 FhG/Risø Model

The FhG/Risø model combines a performance model and an ageing lifetime model. This can be used as shown in Figure 8 below. It is seen how the battery model is included in the complete system model via a battery energy storage system model. The battery energy storage system model includes models of the battery control system as well as the grid interface. The battery energy storage system is a component in a power system model. The power system model models the complete power system including its control. This determines the operating conditions of the battery energy storage system with its own controller.

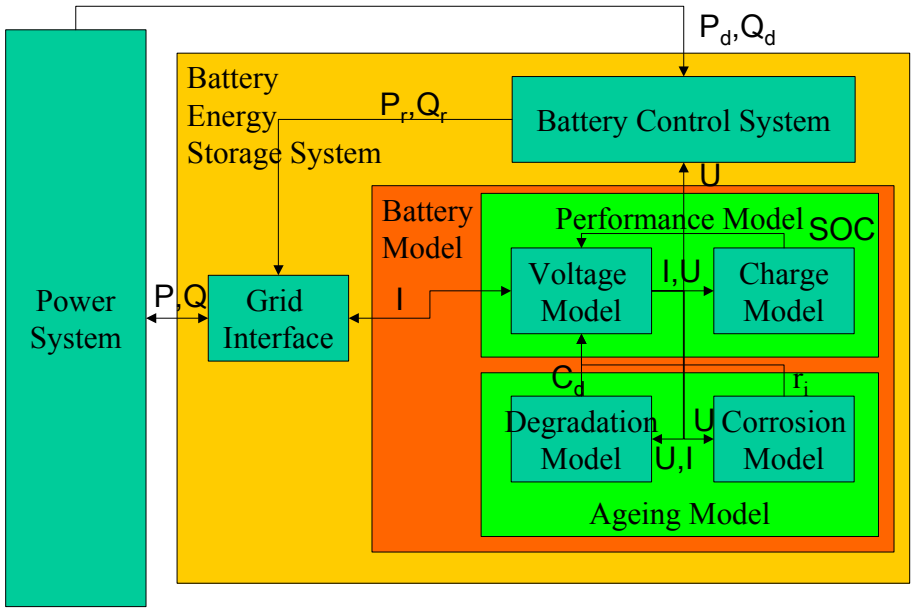

Figure 8 Overview of FhG/Risø combined performance and battery life model

The description of the existing model is based on H.G. Puls, [13], where most equations are derived. The original work is in the model extension and in the validation exercise.

The fundamental equation in the FhG/Risø model is the Shepherd equation which contains parameters that change during the lifetime of the battery to provide an ageing profile and a degradation of the battery performance. The parameters are influenced by various factors including depth of discharge, time at low state of charge and Amp-hours throughput. The initial values for the parameters are obtained from constant current charge and discharge curves, see section 3.1.4. The values of the parameters used in the model to determine a theoretical end of life of the battery are determined using the float life and IEC-cycle life, both of which are taken from the manufacturer's data sheet.

The change in parameters is calculated at every model time step according to a current input and the factors mentioned above. Additionally, at each time step the remaining capacity of a fully charged battery discharged at I_{10} (i.e. the C_{10} capacity) is calculated

and if this falls below 80% of the nominal capacity then the end of the life of the battery is signalled. This repeated program cycle is shown in the flow diagram in

Figure 9.

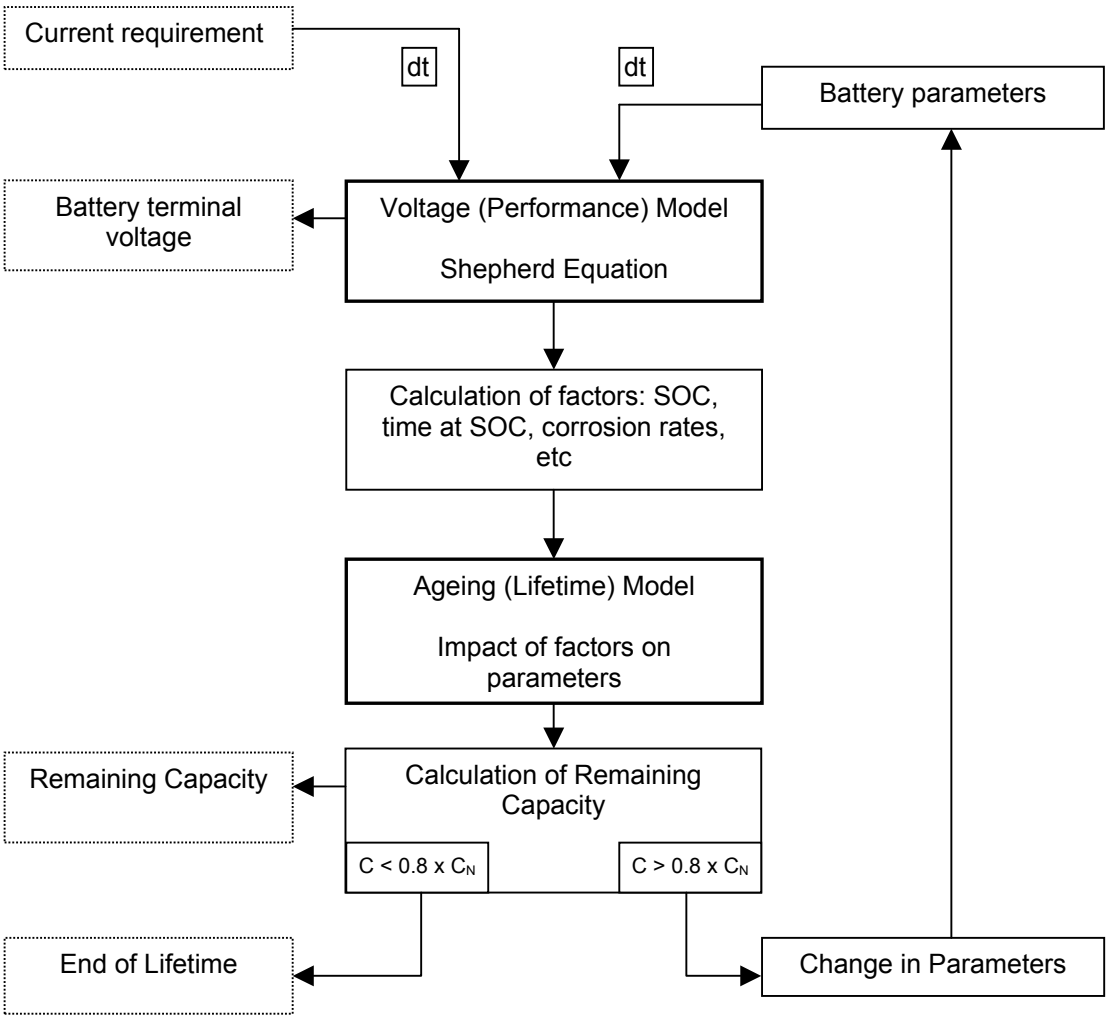

Figure 9 FhG/Risø Battery Model Flow Diagram

5.1 Performance model description

This section describes how the voltage model and ageing model work and how they integrate together to form the whole battery model.

5.1.1 The Voltage Model

The voltage model is based on the Shepherd Equation, which models the terminal voltage of a battery cell. The formulation used in the model (Equations 1 and 2) consists of four terms the first of which is the open circuit, full charge equilibrium voltage i.e. the voltage of the cell when it is fully charged and rested long enough for the electrolyte to reach constant density. The second term is associated with the state

of charge (SOC) of the battery. It is assumed that this term is linear with respect to the depth of discharge (DOD). The third term represents the ohmic losses in the battery through the use of the internal resistance, which is an aggregate value of the various loss mechanisms which are proportional to the current. The major contributors are the grid resistance and the resistance of the electrolyte. The fourth term models the charge factor over voltage and is significant when the battery is very close to being empty or full.
However, several terms are neglected including dynamic terms to model the electrolyte diffusion and the dependence of the resistive elements to the SOC. This is unproblematic. The dynamic behaviour of batteries is not relevant in this context and the dependence of the resistive elements on SOC is both small and, as far as a parameter fit for determining the constants is concerned, is taken into account by the fourth term.

$$U_{cell} = U_{oc} - g_c H + \rho_c \frac{I}{C_N} + \rho_c M_c \frac{I}{C_N} \frac{F}{C_c - F}, \quad I > 0 \qquad \textit{Equation 1}$$

$$U_{cell} = U_{od} - g_d H + \rho_d \frac{I}{C_N} + \rho_d M_d \frac{I}{C_N} \frac{H}{C_d - H}, \quad I \le 0 \qquad \textit{Equation 2}$$

U_{cell}	[V]	terminal voltage of battery cell
F	-	normalised SOC ($Q(t)/C_N$, F <=1)
H	-	normalised DOD (1-F)
I	[A]	charge: I>0, discharge: I<=0
U_{0c}, U_{0d}	[V]	open circuit full charge equilibrium cell voltage
g_c, g_d	[V]	electrolyte proportionality constant
ρ_c, ρ_d	[ΩAh]	aggregated internal resistance
C_N	[Ah]	nominal capacity at standard conditions at the discharge rate I_N, the 10h rate is used in the model.
M_c, M_d	-	charge transfer overvoltage coefficient
C_c, C_d	-	normalised capacity

The subscripts *c* and *d* refer to a charge and discharge operation respectively. Although the Shepherd equation is developed for discharge conditions it is assumed the structure is the same for charge conditions, but with a different set of parameters. The parameters are found from charge and discharge experiments at constant currents as was discussed in section 3.1. In the original Shepherd-based model it was assumed that all the model parameters are constant, both over time and independent of operating conditions.

The voltage model is at the core of the battery performance model. It is the voltage that is used in the control of the battery and it is voltage model parameters that are modified as a result of the ageing modelling.

5.1.2 The Charge Transfer Model

The charge transfer model is used to calculate the SOC of the battery. The main mechanism is that the SOC depends on the time integral of the current. However, depending on the voltage not all the charge is stored as chemical bound charge in the battery, but some is lost due to gassing. The higher the voltage of the battery the more gas is developed and less of the current is actually converted to change of SOC. The model is taken from[13]. The SOC is calculated using

$$F = F_{init} + \int_{t=0}^{t} \frac{I_{SOC}}{C_N} d\tau \quad , \quad I_{SOC} = I - I_{Gas}$$

Equation 3

F_{init} is the initial SOC of the battery. I_{Gas} is calculated using

$$I_{Gas} = \frac{C_N}{100Ah} I_{G0} \exp(c_U (U_{cell} - U_N) + c_T (T_{batt} - T_N)) \quad , \quad I_{Gas} \le I \quad , \quad U_{cell} > U_N$$

Equation 4

I_{G0}	A	Gassing current of a 100Ah battery at nominal conditions ($U_{cell}=U_N$, $T_{batt}=T_N$)
c_u	V^{-1}	Voltage coefficient ($c_u=11V^{-1}$)
c_t	K^{-1}	Temperature coefficient ($c_T=0.06K^{-1}$)
U_N	V	Nominal battery cell voltage ($U_N=2.23V$)
T_N	K	Nominal battery temperature ($T_N=293K$)

The gassing current increases during operation because antimony is released from the positive grid and settles on the negative electrode thus reducing the hydrogen overpotential, which leads to the increase in gassing. It is assumed that the gassing current increases proportionally to the increase in internal resistance.

5.2 Ageing model

There are two ageing mechanisms that are modelled in the FhG/Risø model: corrosion and active material degradation. An overview of the manner in which they are handled is described in this section based on H.G. Puls, [13], where the detailed derivations of the equations are given.

Corrosion in the model is considered as the oxidation of Pb from the grid of the positive electrode into PbO_2 and PbO. This leads to a considerably lower conductivity and lower density of the oxidised lead. The lower conductivity results in higher resistive losses and the change in density develops mechanical stresses in the plate grid. Some parts of the corrosion layer may flake off thus causing active material to lose contact with the grid.

Thus corrosion results in a loss of capacity not only through an increase in internal resistance but also due to loss of active material.

Degradation is also a loss of active material but comes as a result of a restructuring of the active material through the discharging and charging process. With each cycle the active material becomes more crystalline, although remaining chemically the same, thus restricting the pores in the electrodes through which electrolyte flows and the surface area available for the transport of ions. Another impact of the change in structure can be the loss of adhesion of parts of the active mass, which increases the internal resistance and can lead to it breaking away.

Hence, degradation results in a loss of efficiency of the active material and can also lead to a loss of active material itself, both of which mean a reduction in capacity of the battery.

The sudden failure of a battery due to, for example, short circuiting caused by a build-up of detached active material in the bottom of the battery container is not modelled.

The essential basis for the ageing model is that ageing can be represented as changes in the resistance and capacity parameter values, ρ_d, ρ_c and C_d. Furthermore, it is assumed that the parameters at any one time can be determined by the sum of the changes. A flow chart showing the two ageing mechanisms and how they are integrated with the rest of the model is shown in Figure 10.

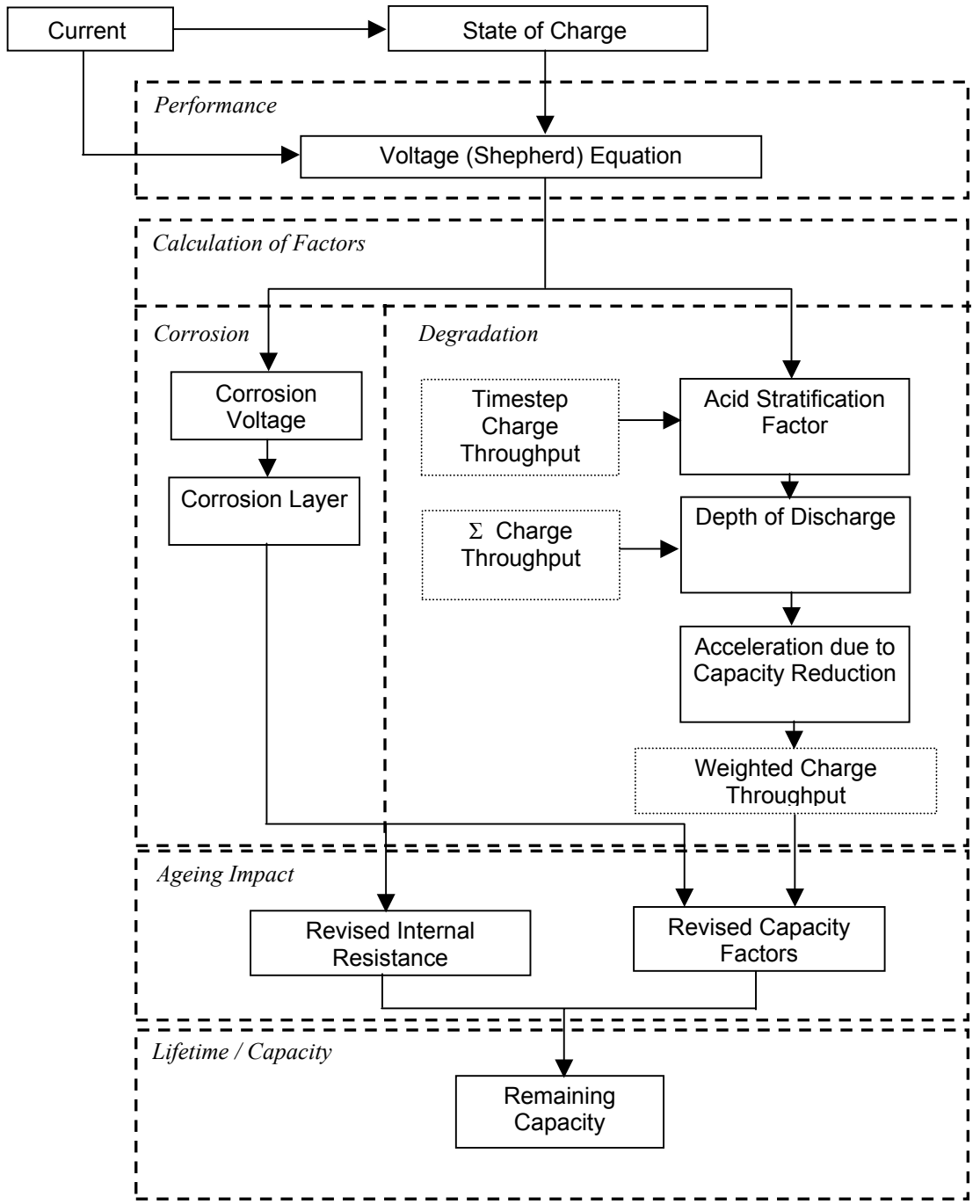

Figure 10 Flow Diagram of Integration of Corrosion and Degradation Processes

5.2.1 Modelling Corrosion

A central facet of the modelling of corrosion in the model is the concept of a corrosion "layer". This is a layer of lower conductivity material that is assumed to grow over the lifetime of the battery. Its resistance is added to the overall resistance of a new battery. The layer is a somewhat theoretical thickness because it also includes an effect of a reduction of active material which has lost contact. The thickness of the layer at time t is designated ΔW_t, and ΔW_{limit} is defined as the layer of corrosion that has been built up at the end of the lifetime of a battery that has been on float charge for all of its life.

The impact of corrosion on the internal resistance and capacity at any time during the battery model simulation is proportional to the ratio of the corrosion layer at that time to the depth of corrosion layer limit, i.e. $\propto \frac{\Delta W_t}{\Delta W_{limit}}$.

5.2.1.1 Calculation of the corrosion layer

The principle for calculation of the corrosion layer is based on work by Lander, [6]. He determined that the voltage of the positive grid with respect to a reference electrode, known as the corrosion voltage, was the key factor in assessing the rate of growth of corrosion, the corrosion speed (k_s). A derivation of his corrosion speed vs. corrosion voltage graph is used in the model and shown in Figure 11.

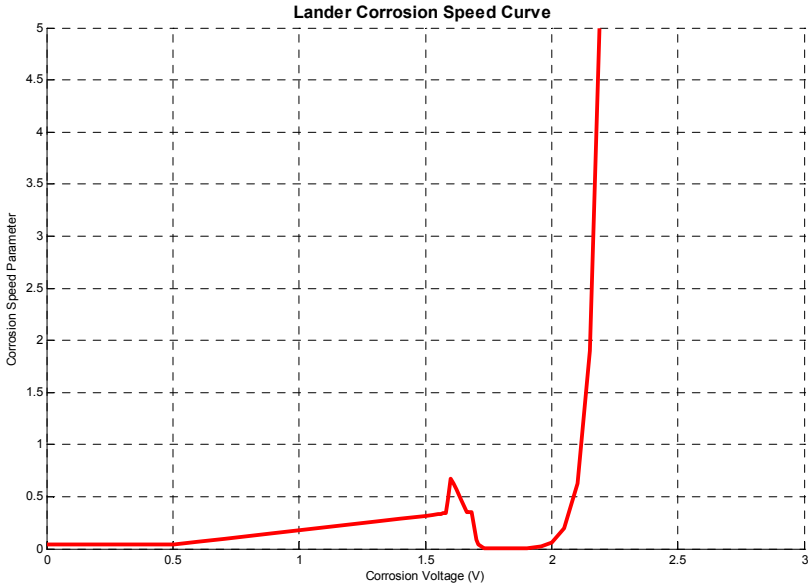

Figure 11 Corrosion speed vs. corrosion voltage (Lander)

The corrosion voltage, U_k, is calculated in the model using a form of the Shepherd equation (Equations 3 & 4) modified to provide just the positive electrode voltage.

$$U_k = U_{k,0}^0 - g_k H + \rho_{c,t}\frac{I_{batt}}{C_N} + 0.5\frac{\rho_{c,0} M_c I_{batt}}{C_N}\frac{F}{C_c - F}, \quad I_{batt} > 0 \qquad \textit{Equation 5}$$

$$U_k = U_{k,0}^0 - g_k H + \rho_{d,t}\frac{I_{batt}}{C_N} + 0.5\frac{\rho_{d,0} M_d I_{batt}}{C_N}\frac{H}{C_{d,t} - H}\ ,\quad I_{batt} \le 0 \qquad \textit{Equation 6}$$

Where $U_{k,0}^0$ = 1.716V, the corrosion voltage without current flow when H=0

g_k = 0.054V, the electrolyte coefficient voltage

Once the corrosion speed parameter has been found from the corrosion voltage, linearized forms of the equations Lander derived for the relationship between the corrosion speed parameter and the existing corrosion layer have been used in the model to find the corrosion layer thickness at a specified time.

$$\left(U_k < 1.74\right)\quad \Delta W_t = k_s \cdot t'^{0.6} \quad where \quad t' = \left(\frac{\Delta W_{t-1}}{k_s}\right)^{\frac{1}{0.6}} + \Delta t \qquad \textit{Equation 7}$$

$$\left(U_k \ge 1.74\right)\quad \Delta W_t = \Delta W_{t-1} + k_s \cdot \Delta t \qquad \textit{Equation 8}$$

5.2.1.2 Calculation of the increase in resistance due to corrosion

It is assumed that the loss of capacity due to the increase in internal resistance and the loss of active mass can be treated separately.

The internal resistance at each time step is assumed to consist of the initial resistance and a contribution from the corrosion (Equation 7).

$$\rho_{d,t} = \rho_{d,0} + \rho_{k,t} \qquad \textit{Equation 9}$$

The increase in resistance during one simulation time step due to corrosion is taken as being proportional to the ratio of the corrosion layer to the depth of corrosion layer limit. The constant of proportionality is the limit of the increase of resistance due to corrosion, $\rho_{k,limit}$.

$$\rho_{k,t} = \rho_{k,limit}\left(\frac{\Delta W_t}{\Delta W_{limit}}\right) \qquad \textit{Equation 10}$$

The limit, $\rho_{k,limit}$, is the increase in internal resistance that is found at the end of the battery's life when on float charge. It is calculated by assuming that 20% of the capacity decrease experienced at the end of life is due to increase in internal resistance. Thus:

$$\rho_{d,end} = \rho_{d,0} + \rho_{k,limit}$$

or

$$\rho_{k,limit} = \rho_{d,end} - \rho_{d,0} \qquad \textit{Equation 11}$$

Where $\rho_{d,end}$ is calculated by reorganising the Shepherd equation:

$$\rho_{d,end} = \left(\frac{C_N}{I_{batt}} \left(U_{cell} - U_{0d} + g_d H \right) - \frac{\rho_{d,0} M_d H}{C_{d,t} - H} \right) - \rho_{d,0} \qquad \textit{Equation 12}$$

Where:

$H = \left(1 - \left(C_{loss} \times F_\rho\right)\right) \times H_0$

$C_{loss} = 0.2$, loss in capacity at end of life

$F_\rho = 0.2$, fraction of loss of capacity due to increase in internal resistance

$U_{cell} = U_{empty}$ *i.e.* $1.8V$

$I_{batt} = -I_{10}$

$C_{d,t} = C_{d,0}$ *i.e.* the there is no capacity loss due to degradation.

5.2.1.3 Calculation of the loss of active mass due to corrosion

The reduction in capacity due to corrosion at any time, t, is calculated as the initial capacity minus the capacity-reducing effect of the corrosion up until that time.

$$C_{d,t} = C_{d,0} - C_{k,t} \qquad \textit{Equation 13}$$

The decrease in active mass during one simulation time step due to corrosion is similarly taken as being proportional to the ratio of the corrosion layer to the depth of corrosion layer limit.

$$C_{k,t} = C_{k,\lim it} \left(\frac{\Delta W}{\Delta W_{\lim it}} \right) \qquad \textit{Equation 14}$$

As 20% of the degradation of capacity at the end of life was due to a resistance increase from corrosion, the degradation of capacity due to loss of active mass from corrosion is taken as 80%. Hence, again by rearranging the Shepherd equation:

$$C_{k,\lim it} = C_{d,0} - \left(H + \left(\frac{\frac{I_{batt}}{C_N} \rho_{d,0} M_d H}{U_{cell} - U_{0,d} + g_d H + \rho_{d,t} \frac{I_{batt}}{C_N}} \right) \right) \qquad \textit{Equation 15}$$

Where:

$H = \left(1 - \left(C_{loss} \times F_c\right)\right) \times H_0$

$C_{loss} = 0.2$, loss in capacity at end of life

$F_c = 0.8$, fraction of loss of capacity due to loss of active mass

$U_{cell} = U_{empty}$ *i.e.* $1.8V$

$I_{batt} = -I_{10}$

$\rho_{d,t} = \rho_{d,0}$

5.2.2 Modelling Degradation

As explained in Section 5.2, degradation is as a result of the charging and discharging process or simply the Ah throughput. As has been used in the corrosion part of the model, the manufacturer's data sheet gives the lifetime of the battery under IEC-cycling conditions. However, this also contains some corrosion effect so the lifetime given is too short for Ah throughput only. Hence, a corrosion-free cycling lifetime, the number of cycles Z, is taken as:

$$Z = 1.6 \times Z_{IEC} \qquad \textit{Equation 16}$$

In a similar process to that in Equation 15, the value of the degradation in capacity at the end of lifetime with Ah throughput cycling only is given by

$$C_{\mathrm{deg,limit}} = C_{d,0} - \left(H + \left(\frac{\frac{I_{batt}}{C_N} \rho_{d,0} M_d H}{U_{cell} - U_{0,d} + g_d H + \rho_{d,t} \frac{I_{batt}}{C_N}} \right) \right) \qquad \textit{Equation 17}$$

Where:

$$H = 0.8 \times H_0$$
$$U_{cell} = U_{empty} \ \textit{i.e.}\ 1.8V$$
$$I_{batt} = -I_{10}$$
$$\rho_{d,t} = \rho_{d,0}$$

An exponential approach, rather than a linear one as used in the corrosion effect, is used for the relationship between the value of degradation at time t and the ultimate limit at the end of life:

$$C_{\mathrm{deg,t}} = C_{\mathrm{deg,limit}} e^{-c_{Z_N}\left(1-\frac{Z_N}{Z}\right)} \qquad \textit{Equation 18}$$

Where:

Z	Cycle life without corrosion
Z_N	Number of nominal cycles experienced at time t
c_{Z_N}	Coefficient of exponential function to determine $C_{deg,t}$ ($c_{Z_N} = 5$)

5.2.2.1 Calculating the number of nominal cycles

The number of nominal cycles is the number of times the nominal capacity has been discharged from the battery. This is, therefore, calculated by summing up all the discharge Ah throughputs, subtracting gassing currents, and dividing that by the nominal capacity.

$$Z_{N,t} = \frac{1}{C_N}\sum_{\tau=0}^{t} I_{Z,\tau} \times \Delta t \qquad \textit{Equation 19}$$

Where:

$$I_Z = \left| I_{batt} - I_{gas} \right| \quad for \;\; I_{batt} \le 0 \;\; \text{(discharging)}$$
$$I_Z = 0 \quad for \;\; I_{batt} > 0 \;\; \text{(charging)}$$

5.2.2.2 The effect of acid stratification

The concentration of the electrolyte changes as part of the chemical processes that take place when the battery is charged and discharged. During repeated cycles a concentration gradient can build up (top to bottom) and the battery then behaves as several batteries of different concentrations working in parallel. Consequently, the charge acceptance is reduced and the capacity deteriorates. In time, the concentration gradients are levelled through diffusion but this takes a very long time. They can be quickly removed by periods of gassing, where the rising bubbles effectively mix the electrolyte resulting in a more homogeneous electrolyte.

The model uses two variables, f_{plus} and f_{minus}, to describe the build up and breakdown of the acid stratification. They are combined to form an overall acid stratification factor, f_s, which takes the value 1 when there is no stratification:

$$f_{s,t} = f_{s,t-1} + (f_{plus} - f_{minus})\Delta t \qquad \textit{Equation 20}$$

The variable f_{plus} is determined using a Fermi distribution profile so that the build up of stratification continues at a certain rate which decreases as the factor increases. This reflects how the development of the stratification decelerates to reach a state of saturation. If the cell voltage is less than the voltage at which stratification decomposition begins (i.e. 2.3v) then $f_{minus} = 0$. If it reaches or exceeds this voltage then f_{minus} is described by an exponential function. The factor will then decrease exponentially when the voltage is high to model the effect of gassing. It also decreases linearly with time.

5.2.2.3 The effect of state of charge

The effect of the state of charge on the ageing of the battery is described by a weighting factor, f_F, which takes the value 1 when the battery is fully charged and grows during phases in between full charges. Growth is proportional to the time elapsed since the last full charge, t_F, and to the lowest state of charge reached during the phase, F_{min}. Thus:

$$f_F = 1 + \left(c_{f,0} - c_{f,\min} \cdot F_{\min}\right) t_F \qquad \textit{Equation 21}$$

Where

$c_{f,0}$ is the increase in f_F per hour at $F_{min} = 0$.
$c_{f,min}$ is the influence of F_{min} on f_F.

5.2.2.4 The total effect on the degradation

The charge throughput for a time step is multiplied by the acid stratification factor, $f_{s,t}$, to give an equivalent charge throughput that would cause the same damage without stratification. This weighted charge throughput is then normalised by the nominal battery capacity to give a stratification-weighted number of cycles for that time step, $\Delta Z_{s,t}$:

$$\Delta Z_{s,t} = f_{s,t}\left(\frac{I_z \Delta t}{C_N}\right) \qquad \textit{Equation 22}$$

Where:

$$I_z = \left|I_{batt} - I_{gas}\right| \qquad for \;\; I_{batt} \le 0$$
$$I_z = 0 \qquad for \;\; I_{batt} > 0$$

Then, for each time step within a cycle between full charges, this stratification-weighted number of cycles is summated and multiplied by the state of charge factor at the present time step. A factor of $1/(1\text{-}C_{deg,t})$ is applied to account for the phenomenon of accelerated degradation as the capacity of the battery decreases. This then gives an equivalent number of nominal cycles that would give the same damage as if there were no corrosion, state of charge impact nor capacity reduction effect.

$$Z_{gn,t} = Z_{gn,tF} + f_{F,t}\sum_{\tau=tF}^{\tau=t}\frac{\Delta Z_{s,\tau}}{\left(1 - C_{deg,\tau}\right)} \qquad \textit{Equation 23}$$

Where:

$Z_{gn,t}$	nominal weighted cycles at the present time step, t
$Z_{gn,tF}$	nominal weighted cycles at the time of the last full charge, t_F
$f_{F,t}$	state of charge factor at current time step, t
τ	time steps between time of last full charge, t_F, and present time step t

The weighted, normalised number of cycles thus gives a representation of the equivalent number of standard cycles that would produce the same degradation effect as the current profile used thus far.

This can then be used to calculate the capacity degradation by substituting Z_N in Equation 18 by Z_{gn}:

$$C_{deg,t} = C_{deg,limit}\, e^{-c_{Z_N}\left(1-\frac{Z_{gN}}{Z}\right)} \qquad \textit{Equation 24}$$

5.2.3 Total effect of capacity reduction

The capacity reduction due to degradation, $C_{deg,t}$, and that due to corrosion, $C_{k,t}$, are then combined to give the capacity factor, $C_{d,t}$, that can be used in the Shepherd equation to produce the battery voltage and the remaining capacity equation to indicate how far the battery has aged.

$$C_{d,t} = C_{d,0} - C_{k,t} - C_{deg,t} \qquad \textit{Equation 25}$$

5.3 Improvements in the model undertaken during the Benchmarking Project

The following changes and improvements were made to the FhG/Risø model during the course of the Benchmarking project:

- Separation from FhG PV system lifetime model.
- Translation onto Matlab platform.
- Data input upgrade.
- Graphic plotting of detailed results.
- High(er) current mechanism modification.
- Corrosion speed profile adjustments.
- Corrosion calculation modifications.
- Low voltage disconnect.

5.3.1 Separation from FhG PV System Lifetime Model

The FhG/Risø battery model was originally part of a model, written in C++, that was designed to evaluate the performance and economics of photovoltaic systems over the whole life cycle of the system. One of the component models was one for lead acid batteries. Under the Benchmarking project FhG separated the battery model from the PV simulation software and Risø took on the task of the verification process using the Benchmarking battery test results and lifetime prediction. It became clear, however, that significant development work was required on the model before it could be used for these purposes predominantly because it was no longer being used within typical low-current PV system limitations.

There therefore followed a series of developmental improvements, mostly using the Benchmarking battery test results, to enable the model to be used in higher current environments.

5.3.2 Translation into Matlab

Although fast, the original code was written in C++. It was decided to translate the model into the Matlab analysis software, [14], a more flexible working environment. This was carried out by Risø together with a verification exercise to guarantee the production of the same results given the same input as the C++ model.

5.3.3 Data input upgrade

The model received from FhG was designed with a front-end user interface that did not allow a time series input of data. The Risø Matlab version was upgraded so that data files of the test data from the Benchmarking battery tests could be handled.

5.3.4 Graphical output of results

In order to facilitate analysis of the results the model was revised to store many of the variables each time step and to produce time series plots.

5.3.5 High current mechanism

Initial model results seriously under predicted the lifetime of the battery. Furthermore, it could be seen that the Ah-weighting factor, discussed in section 5.2, was very large at high currents and was having a disproportionate effect on the lifetime calculation. As the model had only previously been used in photovoltaic systems, where current values are much lower, this effect had not been seen in the model before.

To attempt to address this problem a factor was introduced that calculated the average discharge current over a 36 hour period and was used to modify the effect of the Ah-weighting factor. This was implemented by summing the discharge Ah-throughput at each time step for the previous 36 hours and dividing this by the sum of the time steps that a discharge current occurs. Thus obtaining an "average" discharge current as follows:

$$Q_{sum} = \sum_{\tau=(t-36/\Delta t)}^{t} I_{factor}\Delta t$$

Where $I_{factor} = I_{batt} \;\; if \;\; I_{batt} < 0$

$I_{factor} = 0 \;\; if \;\; I_{batt} \geq 0$

$$T_{sum} = \sum_{\tau=(t-36/\Delta t)}^{t} \Delta\, t_{factor}$$

Where $t_{factor} = \Delta t \;\; if \;\; I_{batt} < 0$

$t_{factor} = 0 \;\; if \;\; I_{batt} \geq 0$

Then

$$I_{factoraverage} = \frac{Q_{sum}}{T_{sum}}$$

This average current is then used to provide a "current factor" which takes the value 1 if the average current is small (I_{100} chosen), 0.1 if the average current is high (I_{10} chosen) and varies in-between for other currents. This also provides a method of tuning whereby the definition of a "high" current can be adjusted so that the impact of the current is correct.

$$f_{currentfactor} = \frac{0.01 C_N}{I_{factoraverage}} \qquad \textit{Equation 26}$$

This factor is then used to modify Equation 20 so that the Ah-throughput factor is adjusted according to the average current:

$$f_{s,t} = f_{s,t-1} + (f_{plus} - f_{\min us})\Delta t\, f_{currentfactor} \qquad \textit{Equation 27}$$

Trial simulation runs showed that this had the desired effect on reducing the rate of the capacity degradation when discharge currents were high.

Some further work is required to tune the averaging period (36 hours is somewhat arbitrary and not related to any known physical processes within the battery), and the multiplying factor in Equation 23 could be refined according to the magnitude of the average current.

5.3.6 Low voltage disconnect

The model calculates the corrosion impact depending on the positive electrode potential and the corresponding corrosion speed. It could be seen that at high rates of discharge the battery model would frequently drop the voltage, and hence positive electrode voltage, down to 0.3V. This was displacing the spread of positive electrode voltages into a region of higher corrosion. A low voltage threshold was thus introduced that disconnected the battery whenever the voltage dipped below 1.75V. This, however, also increased the modelled impact of corrosion because the corrosion rate at 1.75V is much higher than at 0.3V (see Figure 11). This was not the expected result of implementing the controller. However, as the low voltage controller for the test batteries did not have to operate until quite some time into the battery's life, it meant that there was still some other mechanism that the model was not representing correctly.

Nonetheless, it was decided to keep the low voltage controller in as operation of a battery below 1.75V is not good practice and this is the reason for battery voltage controllers being used in real systems.

5.3.7 Corrosion calculation modification

5.3.7.1 Modification of the Corrosion Voltage Equation

Investigation of the corrosion voltage equations (Equations 5 & 6) highlighted a concern over the use of a factor of 0.5 only for the charge factor overvoltage term in calculating the positive electrode voltage. The equations were changed to reflect a better voltage distribution between the positive and negative electrodes.

$$U_k = U_{k,0}^0 - \frac{10}{13} g_k H + 0.5\rho_{c,t}\frac{I_{batt}}{C_N} + 0.5\frac{\rho_{c,0} M_c I_{batt}}{C_N}\frac{F}{C_c - F}, \quad I_{batt} > 0 \qquad \textit{Equation 28}$$

$$U_k = U_{k,0}^0 - \frac{10}{13} g_k H + 0.5\rho_{d,t}\frac{I_{batt}}{C_N} + 0.5\frac{\rho_{d,0} M_d I_{batt}}{C_N}\frac{H}{C_{d,t} - H}, \quad I_{batt} \le 0 \qquad \textit{Equation 29}$$

The factor 10/13 was derived as follows: A typical change of the open circuit voltage from fully charged to 100% discharged is 130mV. Approximately 100mV of this change can be attributed to the positive electrode and 30mV to the negative electrode.

5.3.7.2 Calculation of Corrosion Thickness Limit

In order to calculate, ΔW_{limit} , the original model used the same corrosion speed parameter value for a battery on float voltage for all batteries, independent of their particular characteristics.

It was decided to calculate a corrosion speed parameter that would reflect the particular battery in use. Firstly, the float current, I_{float}, that is necessary to keep a fully charged battery at 2.3V is calculated using a rearranged Shepherd equation with F = 1,

$$I_{float} = \frac{C_N}{\rho_{c,0}\left(1+\frac{M_c}{C_N\cdot(C_c-1)}\right)}\cdot\left(U_{float}-U_{0,c}\right) \qquad \textit{Equation 30}$$

Then the I_{float} is taken to calculate the voltage of the positive electrode from the above equation for the corrosion voltage during charging:

$$U_{k,float,new} = U^0_{k,0} + 0.5\cdot\frac{I_{float}\cdot\rho_{c,0}}{C_N}\cdot\left(1+\frac{M_c}{C_c-1}\right) \qquad \textit{Equation 31}$$

The corrosion speed parameter, k_s, corresponding to this corrosion voltage is obtained from Figure 11 and then used to calculate the corrosion layer limit:

$$\Delta W_{limit} = c_t L_{80\%} k_s \qquad \textit{Equation 32}$$

Where c_t $365\times 24\ [hrs]$

$L_{80\%}$ Float lifetime in years

5.3.7.3 Calculation of Internal Resistance Limit

A revision was made to the calculation of the internal resistance limit (Equation 12) so that the internal resistance limit at the end of life is calculated with respect to the initial capacity of the battery rather than the nominal capacity. This means that H_0* (the DOD for a full discharge of the initial battery) rather than H_0 (the DOD for a full discharge of the nominal battery capacity) is used in Equation 12.

5.3.7.4 Revised Relationship for Growth of Corrosion Parameters

To reflect the reduction in the rate of increase of corrosion as a battery ages the relationships in Equations 10 and 14 have been updated from a proportional one to the following exponential which is intended to reflect the inherent slowing down of a corrosion process with increasing age:

$$\rho_{k,t} = \rho_{k,\text{limit}} \cdot 2 \cdot \left(1 - e^{\frac{\ln\frac{1}{2}}{dW_{\text{limit}}} \cdot dW} \right) \quad \textit{Equation 33}$$

$$C_{k,t} = C_{k,\text{limit}} \cdot 2 \cdot \left(1 - e^{\frac{\ln\frac{1}{2}}{dW_{\text{limit}}} \cdot dW} \right) \quad \textit{Equation 34}$$

5.4 Parameter estimation

To allow for the analysis of the test data parameters were identified for each battery as was discussed in section 3.1.

5.4.1 Parameter fitting methodology

Parameters were required to fit the following version of the Shepherd equation:

$$(I_{batt} > 0) \quad U_{cell} = U_{0c} - g_c H + \rho_{c,t} \frac{I_{batt}}{C_N} + \frac{\rho_{c,0} M_c I_{batt}}{C_N} \frac{F}{C_c - F} \quad \textit{Equation 35}$$

and

$$(I_{batt} \le 0) \quad U_{cell} = U_{0d} - g_d H + \rho_{d,t} \frac{I_{batt}}{C_N} + \frac{\rho_{d,0} M_d I_{batt}}{C_N} \frac{H}{C_{d,t} - H} \quad \textit{Equation 36}$$

where:

U_0	Voltage at full state of charge	V
g	Electrolyte coefficient of the cell voltage parameter	V
H	Depth of discharge	-
ρ	Internal resistance parameter	ΩAh
I	Current	A
C_N	Nominal battery capacity	Ah
M	Activation polarization voltage coefficient	-
C	Capacity coefficient	-
F	State of charge (F = 1-H)	-

0	Initial value
t	Value at time t
c	Charging parameter
d	Discharging parameter

The process of fitting of the parameters to the test data is described below:

- Some parameters are constrained by physical limitations of their representation by the Shepherd equation (for example $C_c \geq 1$ otherwise the battery will not charge to 100% SOC).

- A Matlab script was developed to read in the test data, allow the user to choose the points to fit and then to fit a curve to those points. The function used was a least squares fit.

- An Excel spreadsheet was then used to fine tune values by eye and expert opinion.

5.4.2 Parameter fitting results

The data for the parameter fitting has been taken from tests carried out by ISPRA.

5.4.2.1 OGi Battery

The OGi battery proved difficult to fit for the discharge curves. The results are shown in Figure 12.

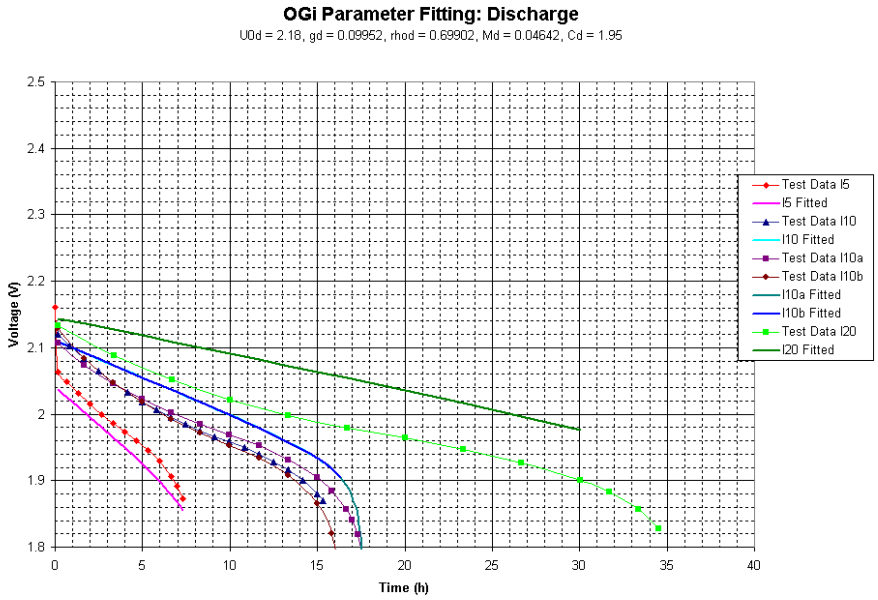

Figure 12 OGi Parameter Fitting: Discharge

As can be seen, none of the curves is very well fitted despite numerous fitting attempts. As part of an investigation to find out why this was the case, the same basic data was plotted but by Ah-throughput rather than time. Figure 13 shows a comparison for four OGi discharge curves all carried out from a full state of charge condition. “I5 ISPRA” was carried out for the purpose of producing an I5 discharge curve. “I10a ISPRA” was carried out next to ensure an empty battery prior to an I5 charge. The “I10 ISPRA” curve is the next chronological test carried out to produce the I10 discharge curve and finally “I10b ISPRA” was done to discharge the battery prior to an I10 charge test. Thus all the discharges represent a discharge from full to the same voltage stop point. From this two things can be seen: 1) that the real capacity of the battery was developing as the tests were being carried out, and 2) that the same capacity was achieved with an I5 discharge and the first I10 discharge.

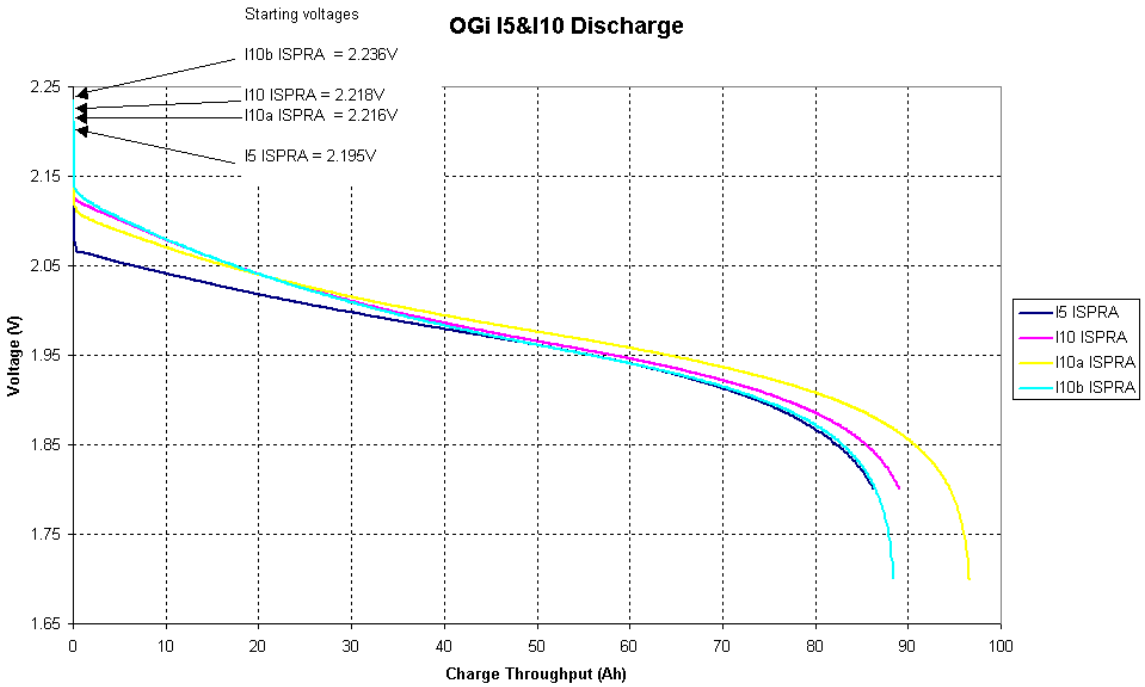

Figure 13 Comparative Charge Throughput for OGi Discharges

This lack of consistency is a large contributory factor in being unable to achieve a good fit for the discharge parameters. Nonetheless, a set of parameters was achieved that represented the best combination of the poorly fitted curves.

The charge curves, however, were fitted easily by the method described above and Figure 14 shows that the parameters are well fitted.

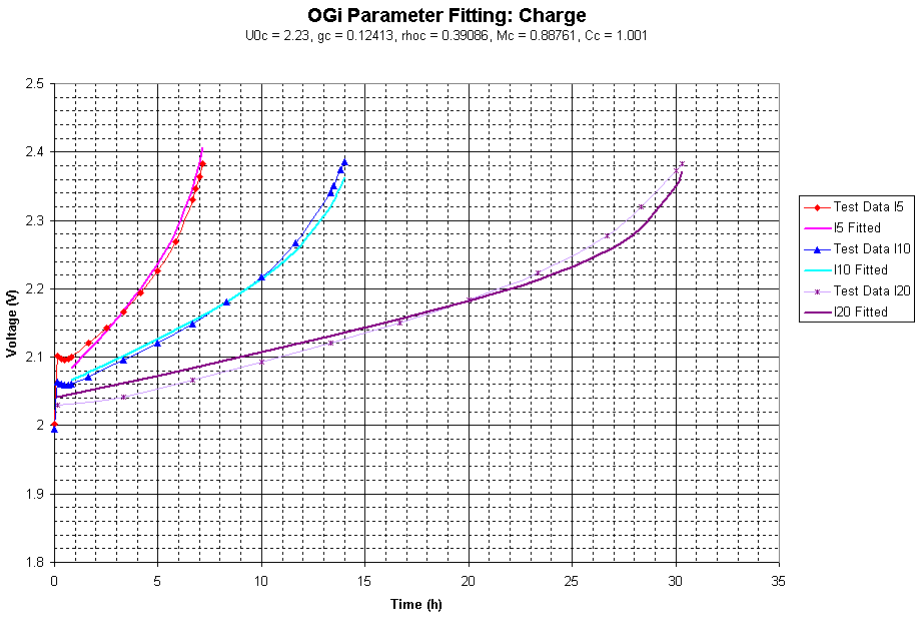

Figure 14 OGi Parameter Fitting: Charge

The parameter values found for the OGi battery are shown in Table 5.

Table 5 Fitted OGi Shepherd Equation Parameters

U_{0d}	2.18 V
U_{0c}	2.23 V
g_d	0.09952 V
g_c	0.12413 V
ρ_{0d}	0.69902 ΩAh
ρ_{0c}	0.39086 ΩAh
C_N	54 Ah
M_d	0.04642
M_c	0.88761
C_d	1.95
C_c	1.001

5.4.3 OPz battery

In comparison to the OGi battery, the OPz battery parameters were relatively easy to fit for both discharge and charge sequences. Figure 15 and Figure 16 show the discharge and charge fitting curves respectively.

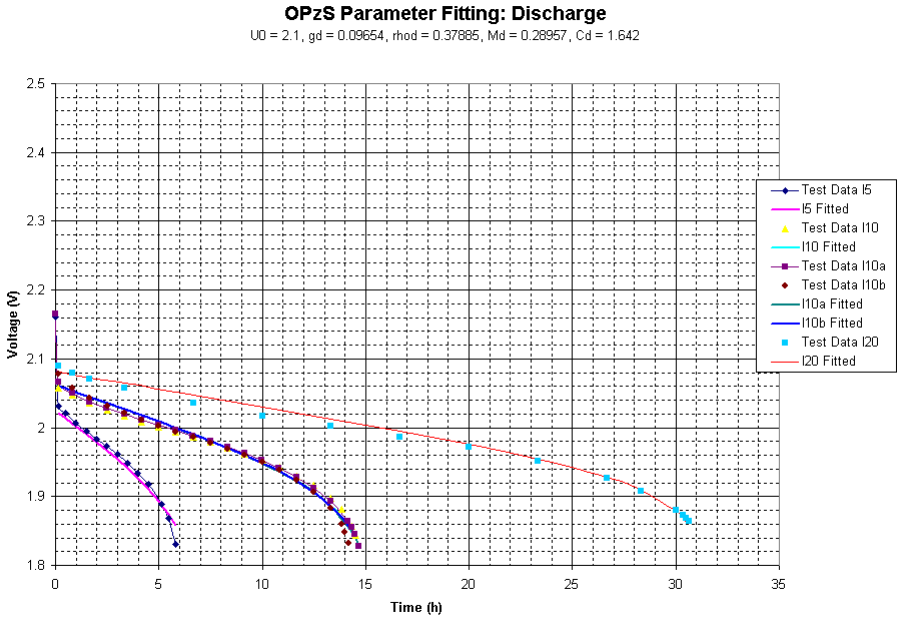

Figure 15 OPz Battery Parameter Fitting: Discharge

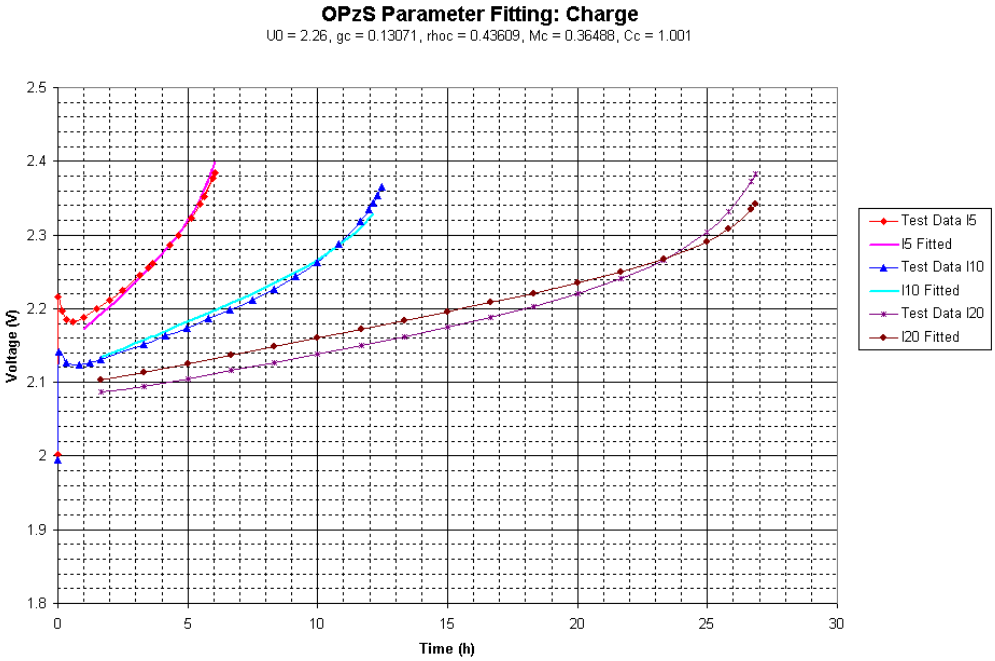

Figure 16 OPz Battery Parameter Fitting: Charge

The parameter values found for the OPz battery are shown in Table 6.

Table 6 Fitted OPz Shepherd Equation Parameters

U_{0d}	2.1 V
U_{0c}	2.26 V
g_d	0.09654 V
g_c	0.13071 V
ρ_{0d}	0.37885 ΩAh
ρ_{0c}	0.43609 ΩAh
C_N	50 Ah
M_d	0.28957
M_c	0.36488
C_d	1.642
C_c	1.001

5.5 Comparison with measurements/test results for validation

Although the FhG/Risø model uses the ageing factors to calculate the impact on the performance, it makes it easier to understand if the performance and ageing are considered separately when analysing the function of the model. The following results come from the CRES tests, putting one of each battery type (OGi and OPz) through each of the profiles (PV and Wind) described in section 3.2.

5.5.1 Performance

In order to look at only the (voltage) performance of the model, it is necessary to limit the discussion to just the initial part of the battery tests where the influence of ageing on the battery parameters is minimised.

The voltage response to the initial cycling procedure carried out to "exercise" the OGi battery prior to the PV profile test is shown in Figure 17. It should be noted that the model battery had a voltage controller limiting the voltage to 2.45V whilst the test battery was operating uncontrolled. Up until 2.45V, the voltage appears to be quite well replicated by the model, although it is expected that this would be the area of model's best performance as the initial cycling is carried out at I10 currents, the current level that the model is built upon. It can also be seen that the model voltage during charge fits better than during discharge, which is to be expected as this is where the battery parameters fitted best.

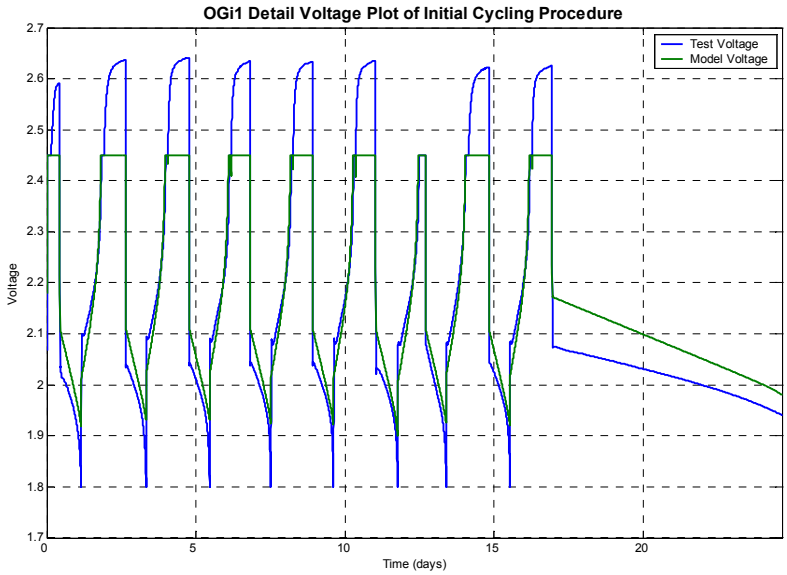

Figure 17 OGi1 Detail Voltage Plot of Initial Cycling Procedure for the PV Test

Figure 18 shows the voltage performance during a section of the first PV profile test for the same OGi battery as described above.

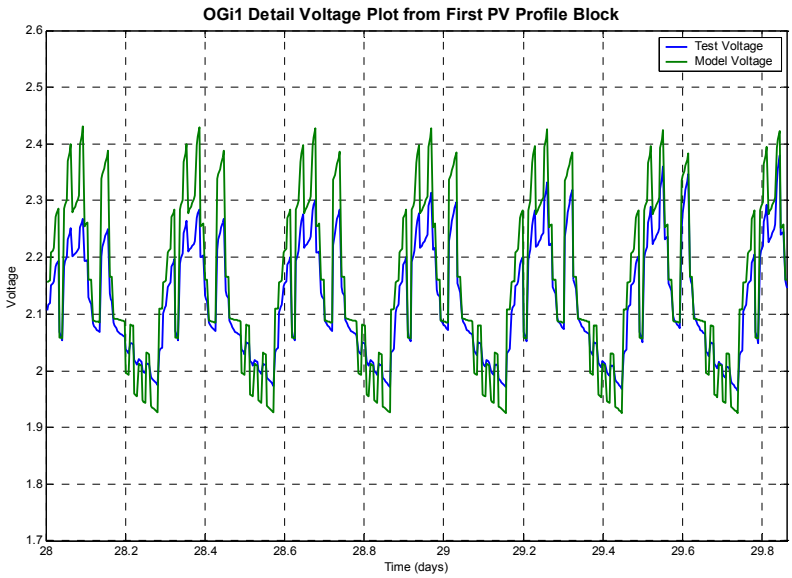

Figure 18 OGi1 Battery Detailed Voltage Plot in First PV Profile Block

Most notable is the over prediction of the voltage swings during charge and discharge parts of the cycle. That is, the model tends to over predict the voltage during charging and under predict during discharging. This implies that the internal resistance term is somewhat high. It is also worth pointing out that the model voltage is similar from cycle to cycle whereas the test battery changes. Although further investigation is required one possible explanation is that the capacity performance changes that occur with acid stratification are not accounted for in the model (the capacity influence is only seen in the ageing process) whereas this is reflected in the test battery as a change in the voltage profile from one cycle to the next.

For the OPz battery, the respective plots are shown in Figure 19 and Figure 20.

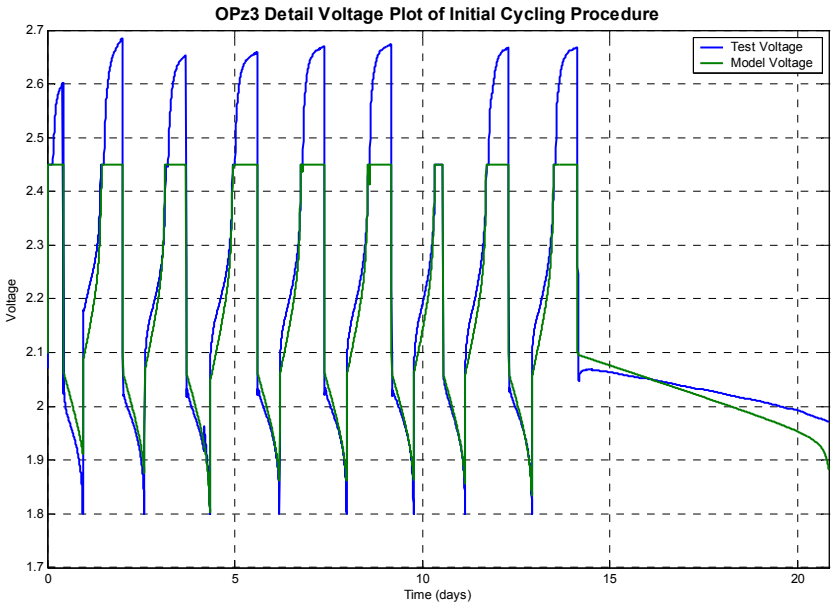

Figure 19 OPz3 Battery Detail of Voltage From Initial Cycling Procedure

The initial cycling procedure (Figure 19) again looks reasonable although slightly worse on the charge sections than the OPz battery. However, attention should be drawn to the longer discharge starting at approximately day 14 which is a low current discharge (approx I100) and this illustrates how the model is not good at simulating currents that are far away from I10. In this case the test battery voltage holds up better than the model as it is characteristic of lead-acid batteries that the effective capacity is higher at lower discharge rates.

The section taken during the first period of the wind profile test is shown in Figure 20 and shows that the OPz simulation responds better than the OGi. However, it is noticeable that the model now tends to under predict at higher charge/discharge rates and over predict at lower discharge rates. This would imply some current sensitivity is required.

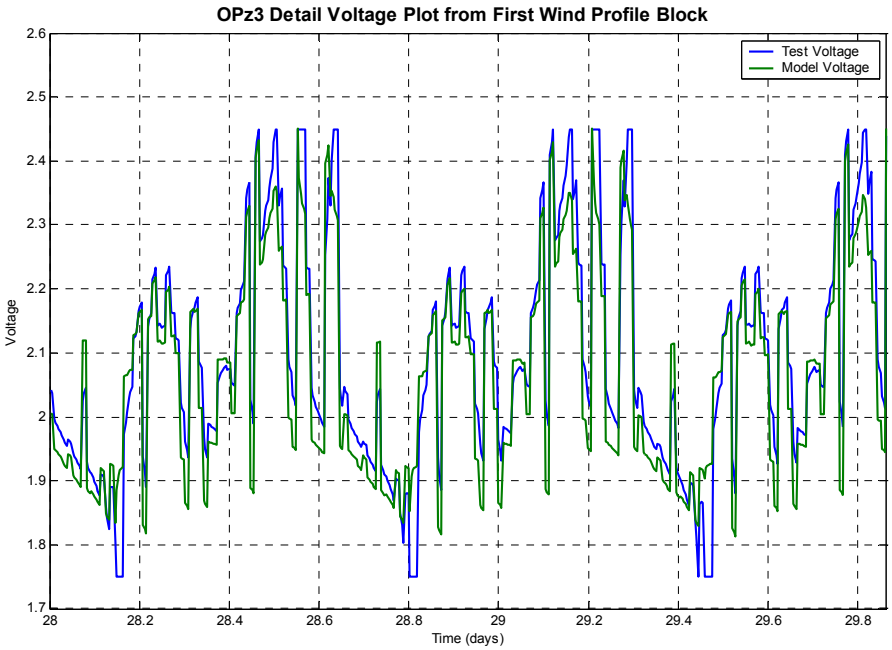

Figure 20 OPz3 Battery Detail Voltage During First Wind Profile Bloc

5.5.2 Lifetime, degradation and aging

The lifetime results of the latest simulations are shown from Figure 21 to Figure 28. Each figure gives three plots:

1) Remaining capacity and state of charge. The remaining capacity is calculated by the model at the end of each time step and the plot shows the overall effect of the development of the ageing process during the battery's lifetime. For comparison, the capacity of the corresponding battery under test at CRES has been plotted. This capacity is measured at the end of each period of cycles. The plot also shows the time trace of state of charge that the model predicts.
2) Model voltage. The cell voltage as calculated by the model is plotted at the start of each time step.
3) Battery current. This shows the current in and out of the model battery in comparison to the test battery. Although there are differences between the model and the test due to discrepancies in the model parameters, it is likely that the battery controllers also work in different ways, giving rise to a difference in the currents.

As an accompaniment to each of the main figures there is also a plot of the capacity factors that are used within the model. These show the development of the various mechanisms modelled by the simulation that go to make up the decline in capacity over the lifetime of the battery. The key for these capacity factors is as follows:

Cdges	Remaining discharge capacity coefficient ($C_{dges} = C_d - C_{deg} - C_k = C_{d,t}$)
Cd	Initial discharge capacity coefficient
Cdeg	Capacity coefficient reduction from degradation process
Ck	Capacity coefficient reduction from corrosion process
rdges	Internal resistance ($rdges = \rho_{d,t}$)
rk	Increase in internal resistance from the corrosion process

5.5.2.1 OGi1 PV Profile

The results for the lifetime simulation of the OGi battery with the PV profile are shown in Figure 21.

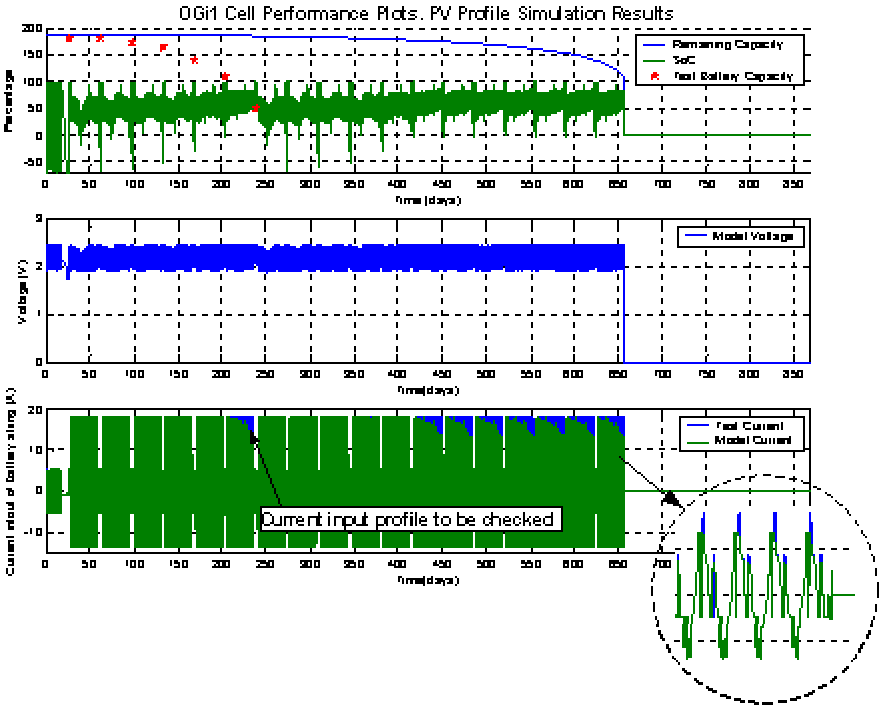

Figure 21 OGi1 Battery PV Profile Results

It can be seen clearly from the top diagram in Figure 21 that the model overestimates the lifetime of the battery in comparison with the test battery results. There could be many reasons for this and these are discussed in the summary of results in section 5.5.2.5 and the findings section 7. The middle diagram shows the voltage of the model battery, whilst the bottom diagram shows the test battery current in blue and the model current in green. The enlargement shows that the test current is plotted as continuing throughout the model simulation for comparison only. In this way it highlights the action of the two battery controllers. It should be noted that it appears that the battery controller in the model has unexpectedly intervened at around 210 days to reduce the charging current. It is suspected that there is some error in the input data and should be checked. However, the model does show a decline in capacity during the lifetime and the contribution of the various capacity factors is shown in Figure 22.

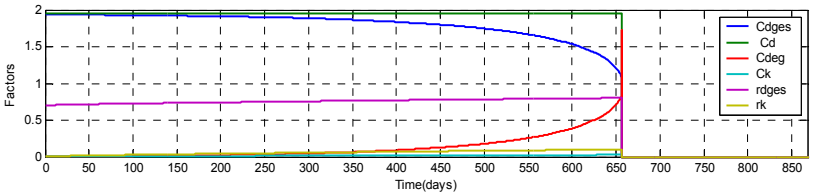

Figure 22 OGi1 Battery PV Profile Capacity Factors

This shows that the greatest contribution to the reduction in capacity is degradation with corrosion only taking a small part.

5.5.2.2 OGi2 Wind Profile

Figure 23 shows the same type of battery subjected to the wind profile test. Again, the model over predicts the lifetime. The current profile plot shows that the model's battery controller is reducing the charging current after approximately 120 days. Looking at the bottom diagram in Figure 23 it is noticeable, however, that that there is a rejuvenation effect in the model from the intermediate capacity tests. This can be seen from the ability of the battery model to accept the full charging current immediately after a capacity test whereas before a capacity test the battery controller had to cut in to limit the charging current.

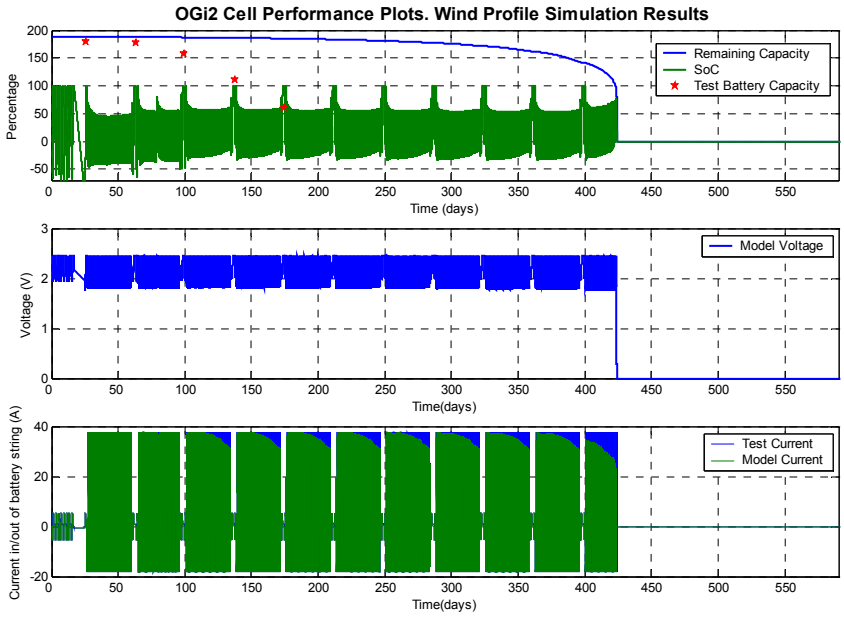

Figure 23 OGi2 Wind Profile Simulation Results

The capacity factors shown in Figure 24 indicate that, as expected, the corrosion plays an even smaller part than with the PV profile merely because the lifetime is shorter and the corrosion layer has had less time to grow.

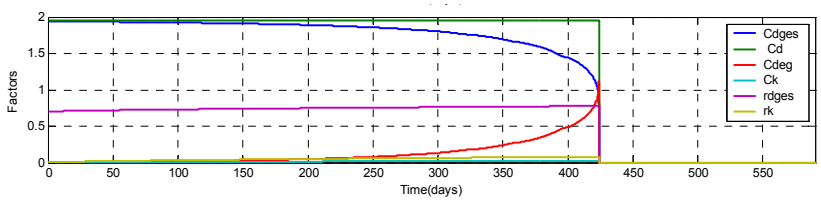

Figure 24 OGi2 Wind Profile Simulation Capacity Factors

5.5.2.3 OPz1 PV Profile

The results from the battery type OPzS PV profile simulation are shown in Figure 25. The battery under test at CRES had not, however, failed at the time of the

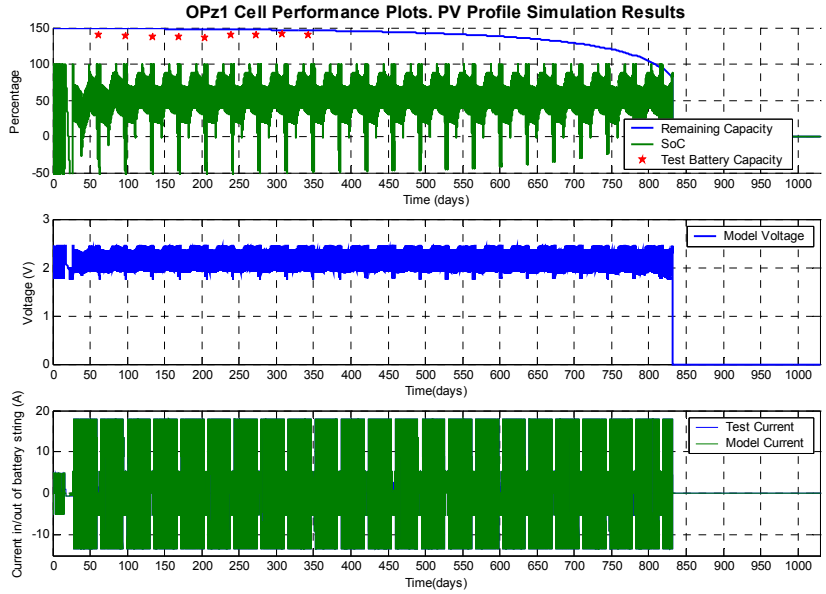

Figure 25 OPzS Battery PV Simulation Results

simulation and it is difficult to make a truthful comparison. This is particularly difficult to extrapolate the test results as it appears as if the battery has recently just gone through a period of conditioning i.e. the capacity has actually increased, a common feature of lead-acid batteries. It is also worth noticing that the battery controller has not had to limit the charging current with this battery and profile. Once again, the capacity factors are shown in Figure 26.

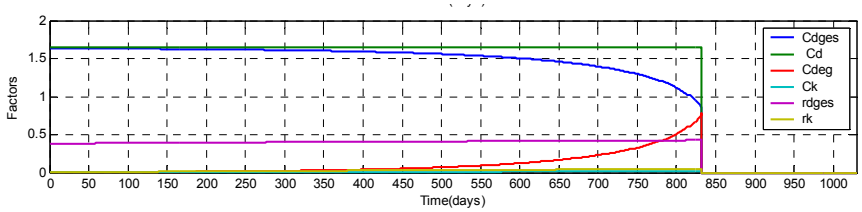

Figure 26 OPz Battery PV Simulation Capacity Factors

5.5.2.4 OPz Wind Profile

Figure 27 shows the OPzS battery simulation and test results from the wind profile. The predicted lifetime is, once again, longer than the test shows. The remaining capacity plot does not show the conditioning effect of the battery as it is a process not modelled in the simulation.

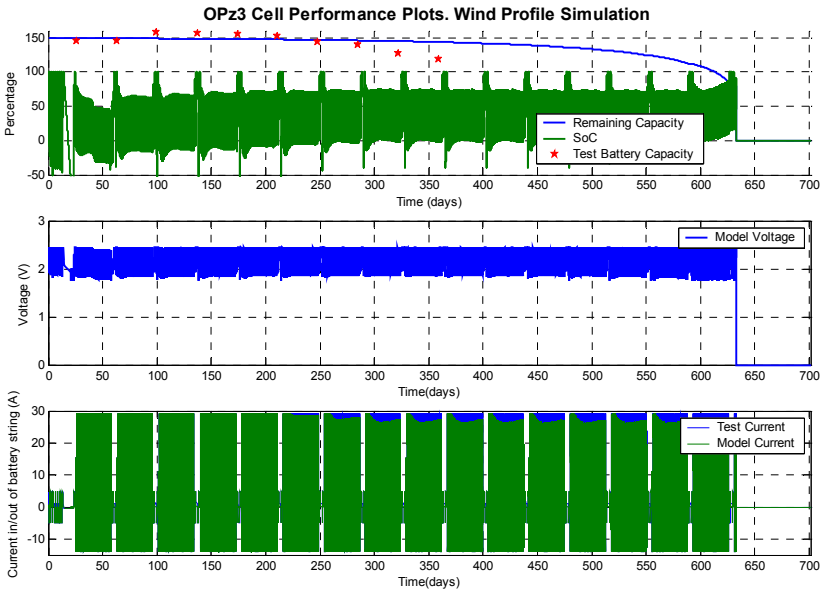

Figure 27 OPz3 Battery wind Profile Simulation Results

The controller in the battery model has restricted the charging current after approximately 210 days. It appears that the regenerative effect of the capacity tests is not as marked as with the OGi batteries because the battery model controller cuts in sooner after the intermediate capacity test has ended.

Once again, Figure 28 shows that the degradation has a much larger contribution to the reduction in capacity compared to the corrosion.

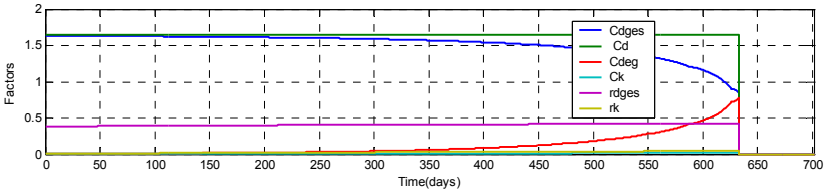

Figure 28 OPz3 Battery Wind Profile Simulation Results

5.5.2.5 Summary of Results

A summary of the results both model simulation and the battery lifetime tests is given in Table 7.

Table 7 Summary of Simulation and Test Results

Battery & Profile	Simulation Lifetime (days)	Test Lifetime (approx days)
OGi1 PV	660	239
OGi2 Wind	425	174
OPz1 PV	830	600+*
Opz3 Wind	633	400*

* = *estimated lifetime(test not yet complete)*

It can be seen that the present model significantly over predicts the lifetime of all of the batteries in all of the tests.

However, the model does correctly predict that the wind profile is harsher than the PV profile, although this is to be expected simply because the wind profile has a higher Ah throughput than the PV. It also correctly predicts that the OPz battery will last longer than the OGi battery, under both PV and wind profiles.

It should be noted that the test lifetime of the OGi battery was markedly shorter than would have been predicted from comparing the respective IEC-cycle lifetimes with the OPz battery. That is, if the OPz battery lasts 420 days under the wind profile cycling then using the IEC-cycle ratio of 1200 (OPz) : 1000 (OGi) then it would be expected that the OGi battery would last 350 days. However, it only managed about half that at 174 days. There is clearly a mechanism at work that is not exercised by the IEC profile. As the model uses IEC-cycle data for basic parameters it is not a surprise that the simulation results do not mirror the lifetime ratio of the test batteries. This is confirmed by the ratios shown in Table 8.

Table 8 Summary of Results with Ratio Comparisons

Profile Type	Test Batteries		**Ratio**	Simulation		**Ratio**
	OGi	OPz		OGi	OPz	
IEC	1000	1200	**1.2**	2001	2500	**1.2**
PV	239	700*	**2.9**	660	830	**1.3**
Wind	174	400*	**2.3**	425	633	**1.5**

* = *estimated lifetime(test not yet complete)*

6 UMass Model

6.1 Model description

The UMass battery model, also known as the Kinetic Battery Model, consists of all three battery models discussed previously; a capacity model, a voltage model and a lifetime model. The models are a mixture of a physically based underlying structure, using constants determined from test data. The capacity model is based on the assumption of a first order chemical rate process. The voltage model is based on the adaptation of the Battery Energy Storage Test (or "BEST") model, in combination with capacity estimates from the capacity part of the model. The lifetime model was initially based on the assumption that the number of cycles a battery can tolerate is a function only of the depth of discharge of the cycles. The lifetime model was adapted to be able to consider random cycling patterns by using a rainflow cycle counting routine. The cycle counting algorithm used is the one commonly used in predicting fatigue damage of materials.

The capacity and voltage portions of the model rely on the assumption that the battery can be considered to be a current source in series with an internal resistance, R_0, as illustrated in Figure 29 below. The voltage of the current source is E, whereas the voltage at the battery terminals is V:

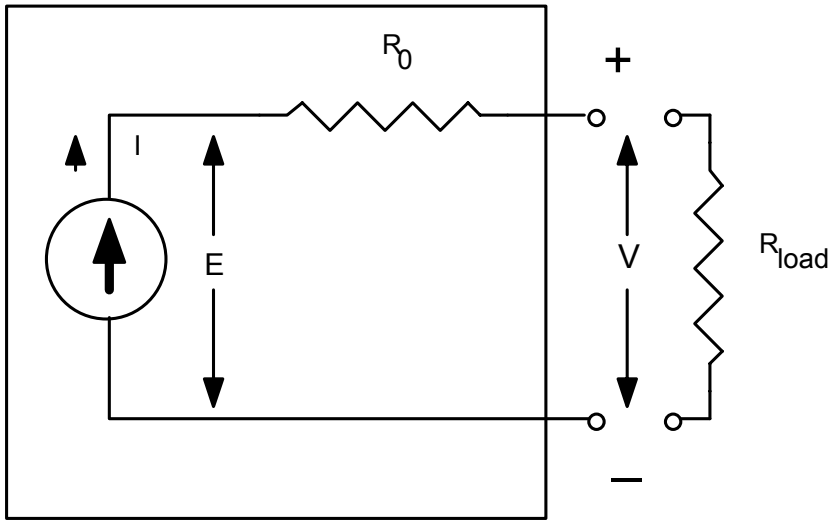

Figure 29 Simple Battery Model Equivalent Circuit

The terminal voltage is then given by:

$$V = E - I R_0 \qquad \textit{Equation 37}$$

The original capacity model was described in Manwell and McGowan (1993), [16]. The development of the voltage portion is described in Manwell and McGowan (1994), [17]. The entire battery model in its most recent form, including the original lifetime portion, is described in the Hybrid2 Theory Manual, [2].

6.2 Improvements in the model undertaken during the Benchmarking Project

The battery model that was used as a starting point for the Benchmarking Project was the form that had been implemented in Hybrid2 software, [2]. The original theory was, however, somewhat more comprehensive than that actually coded into Hybrid2. Accordingly, part of the work described below involved separating the battery model from Hybrid2 and then giving it its full capability, before adding new features.
The work completed under the Benchmarking Project included the following tasks:

- The battery model was separated from Hybrid2, and a free-standing version of same has been prepared. The working name of this model is "KiBaMBatteryModel.exe".
- A computer code capable of estimating model parameter has been written. This is a separate piece of software, which uses data from constant current charge or discharge tests to estimate the three capacity constants and the eight voltage constants. The working name of this code is "BatteryParameterFinder.exe".
- The rainflow cycle counter has been enhanced to allow the mean of the cycles to be accounted for as well as the cycle depth. Lifetime predictions can now be done by taking into account these means. Since relevant lifetime data is typically not available, an estimation method has been suggested which allows adjusting the predictions.
- The rainflow cycle counter has been further investigated to allow charge or discharge rates to be accounted for as well as depth and cycle mean. The results have been very promising to date, but the final form of this counter has not been completed. It must be noted that even when it is completed, it will only become generally useful when more test data relating battery life to charge or discharge current is available. Modifications to the rainflow cycle counter are described in more detail below.

6.3 Parameter estimation

Each of three parts of the UMass battery model requires some experimental data to estimate the parameters.

6.3.1 Capacity Model

The capacity model, which describes the capacity as a function of current, $q_{\max}(I)$, is of the following form.

$$q_{\max}(I) = \frac{q_{\max,0}\, kcT}{1 - e^{-kT} + c\left(kT - 1 + e^{-kT}\right)} \qquad \textit{Equation 38}$$

The capacity model has three constants:

$q_{\max,0}$ = Maximum capacity (at infinitesimal current), Ah
k = Rate constant, hrs^{-1}
c = Ratio of available charge capacity to total capacity, -

The three constants, $q_{max,0}$, k and c may be found by non-linear curve fitting routine from test data. The required data in this case is battery capacity as function of charge or discharge current. The data must be obtained from constant current charges or discharges.

A typical capacity vs. current curve is illustrated in Figure 30 below

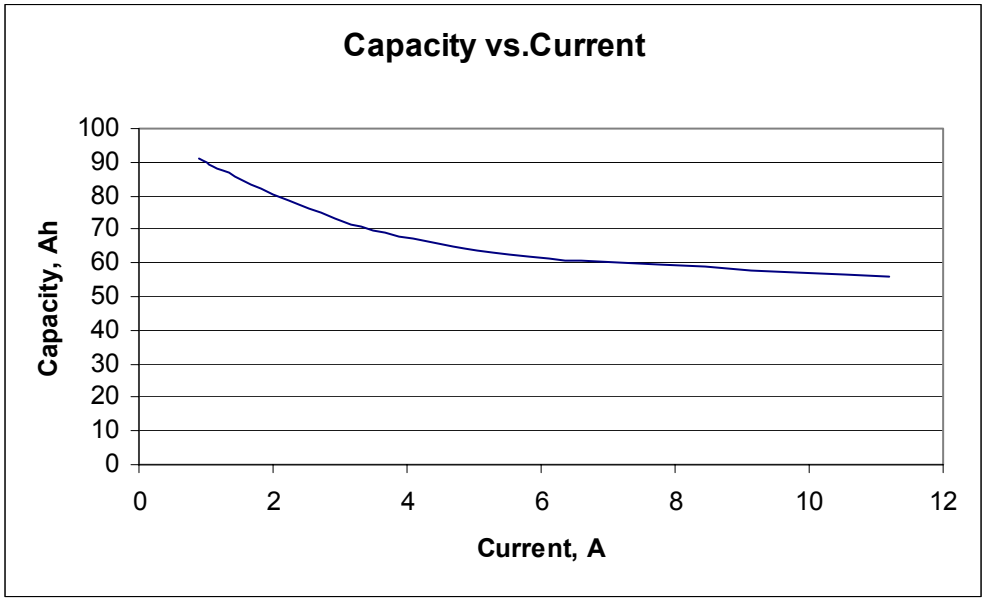

Figure 30 Typical Capacity vs. Discharge Current Relation

6.3.2 Voltage Model

The voltage model is of the form:

$$E = E_0 + AX + CX/(D - X) \qquad \textit{Equation 39}$$

where

E_0 = Fully charged/discharged internal battery voltage (after the initial transient)

A = Parameter reflecting the initial linear variation of internal battery voltage with state of charge. "A" will typically be a negative number in discharging and positive in charging, but it need not be so.

C = Parameter reflecting the decrease/increase of battery voltage when battery is progressively discharged/charged. C will always be negative in discharging, positive in charging.

D = Parameter reflecting the decrease/increase of battery voltage when the battery is progressively discharged/charged. D is positive and is normally approximately equal to the maximum capacity. However, the nature of the fitting process will usually be such that it will not be exactly equal to that value.

X = Normalized maximum capacity at the given current.

The normalized maximum capacity, X, in charging is defined in terms of the charge in the battery by:

$$X = q / q_{\max}(I) \qquad \textit{Equation 40}$$

In discharging, X is defined in terms of the charge removed by:

$$X = \left(q_{\max}(I) - q\right) / q_{\max}(I) \qquad \textit{Equation 41}$$

The voltage model reflects the observations that terminal voltage depends on:

1) State of the battery (charging or discharging)
2) State of charge of the battery
3) Internal resistance of the battery
4) Magnitude of the charging or discharging current.

The values of the eight voltage parameters (four each for charging and discharging), E_0, A, C, D may be found using a non-linear curve fitting routine. The required data is voltage vs. time for constant current charges or discharges. At least four sets of tests are typically used for either charging or discharging. Examples of how constants are obtained are provided below.

6.3.3 Lifetime Model

The lifetime model uses a double exponential curve fit to commonly available cycles to failure vs. cycle depth data. The equation used is of the following form:

$$C_F = a_1 + a_2 e^{-a_3 R} + a_4 e^{-a_5 R} \qquad \textit{Equation 42}$$

where:

C_F = Cycles to failure
a_i = Fitting constants
R = Range of cycle (fractional depth of discharge; normalized using $q_{max,0}$).

Because battery state of charge does not typically follow a regular cycling pattern, a cycle counting algorithm is used to identify cycles. The cycle counting portion of the lifetime model is based on that proposed for material fatigue by Downing and Socie (1982), [18], and is known as rainflow cycle counting. A two-step approach is applied to a state of charge time series. First, an algorithm is applied to identify relative high and low points (peaks and valleys), resulting in a new, and shorter, time series. Then a second algorithm is applied to the time series of peaks and valleys to find the individual cycles. After the cycles have been identified they are counted into bins. The bins correspond to different depths of discharge, with the final bin corresponding to complete discharge and recharge from a full battery. The total discharge range is divided into equal size bins, and at least 20 bins are typically used. The present form of the cycle counting aspect of the model is described in more detail below.

6.3.4 Modified Rainflow Cycle Counter

The modified rainflow cycle counter identifies individual cycles in a time series in the same way as the original cycle counter. In the modified counter, the mean SOC of each cycle is determined from the average of the values of the points at the

maximum and minimum of the cycle. The mean of the cycle is stored in a vector, together with the range of SOC for each cycle. These values are then used in a two dimensional binning procedure to give the number of occurrences of various values of ranges and means within a specified range. For tracking cycle discharge rates, the time step of each peak and valley identified in the initial part of the algorithm is saved and carried along with the value of the peak or valley. This allows the time elapsed in both the charging and discharging part of the cycle to be calculated. With the change in charge and the time elapsed it is possible to calculate the average charging or discharging current. At present, the discharging current is calculated and saved. With this, a three dimensional binning can be performed. For convenience this may be displayed as histograms in either of three different spaces: cycle range, cycle mean, and rate of discharge. Examples are provided below.

In the modified battery lifetime model, adjusted constants can presently only be obtained by inference, using actual test results in combination with simulations. Note that at this point, only the means (in addition to the ranges) are considered-discharge rates are not presently used.

The method for including the effect of mean cycle depth is as follows. It is assumed that (1) lifetime data supplied by a manufacturer is based on cycles starting with a full battery, (2) the effect of lower mean cycles (i.e. cycles starting when the battery is already partially discharged) varies linearly from the lowest possible cycle mean (for cycles of given magnitudes) to that of a cycle starting and ending full, and (3) a reasonable low mean reference life is given by a straight line, whose magnitude, $C_{F,R,}$ is constant and equal to the asymptotic lowest life in the original curve. Then, a new lower limit life curve can be found such that:

$$C_{F,L} = F\left(C_F - C_{F,R}\right) + C_{F,R} \qquad \textit{Equation 43}$$

where F is a life curve adjustment factor between 0 and 1.

The new curve corresponds to the cycles to failure for any cycles that go between fully discharged and some higher value. Three typical curves are illustrated in Figure 31.

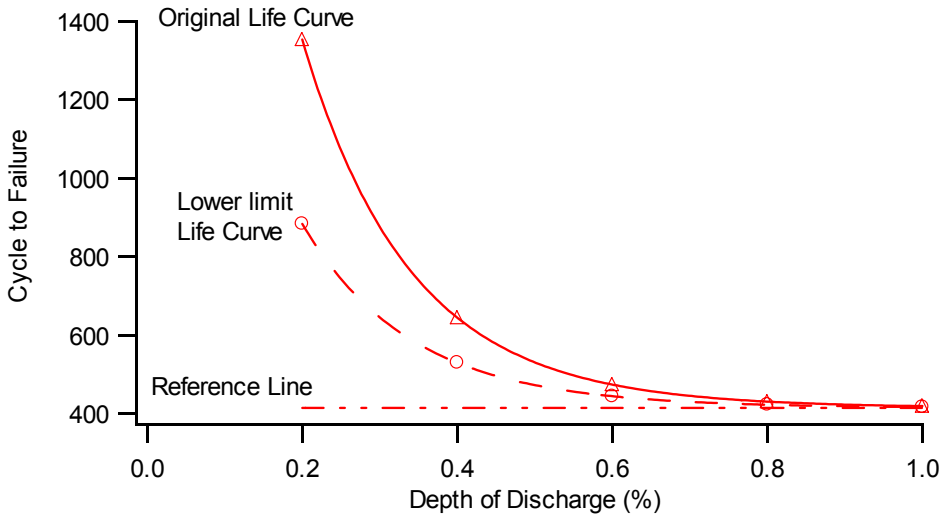

Figure 31 Sample Original and Lower Limit Cycles to Failure Curves. The original life curve gives the number of cycles which can be carried out starting from a full battery and the lower limit life curve gives the number of cycles which can be carried out when each cycle reaches the lowest possible SOC during a cycle

The two upper curves are used by identifying the actual mean, m_{act}, the highest possible mean, m_{high}, which is starting from a fully charged battery, and the lowest possible mean, m_{low}, which is a cycle where the discharge event ends with a completely discharged battery, for each cycle. Consider a cycle with range R_i. The highest normalized mean is 1-R_i/2. The lowest normalized mean is R_i/2.

The adjusted cycle to failure for this cycle, $\hat{C}_F$, is given by:

$$\hat{C}_F = C_F - \left[C_F - C_{F,L}\right]\left[\left(1 - R_i/2 - m_{act}/q_{\max,0}\right)/\left(1 - R_i\right)\right] \qquad \textit{Equation 44}$$

Note that the value of F is obtained by applying the above equation in such a way that the predicted lifetime is equal to that of the test data. Thus the predicted result can be as close as desired to the test data, provided that an F can be found that fits within the expected range of 0-1. The supposition then is that the resulting lower limit curve and original curve can be used in subsequent simulations and give results that are closer than they would be, assuming that only the original curve were used.

6.3.5 Determination of Constants

The following example illustrates the determination of constants for the OPzS battery.

6.3.5.1 Capacity and Voltage Constants

Voltage vs. charge removed data for constant current discharge tests are illustrated in Figure 32. The figure is a screen from the input data section of BatteryParameterFinder.exe. Note that charge removed is obtained from elapsed time multiplied by the current. The corresponding charging curve is shown in Figure 33.

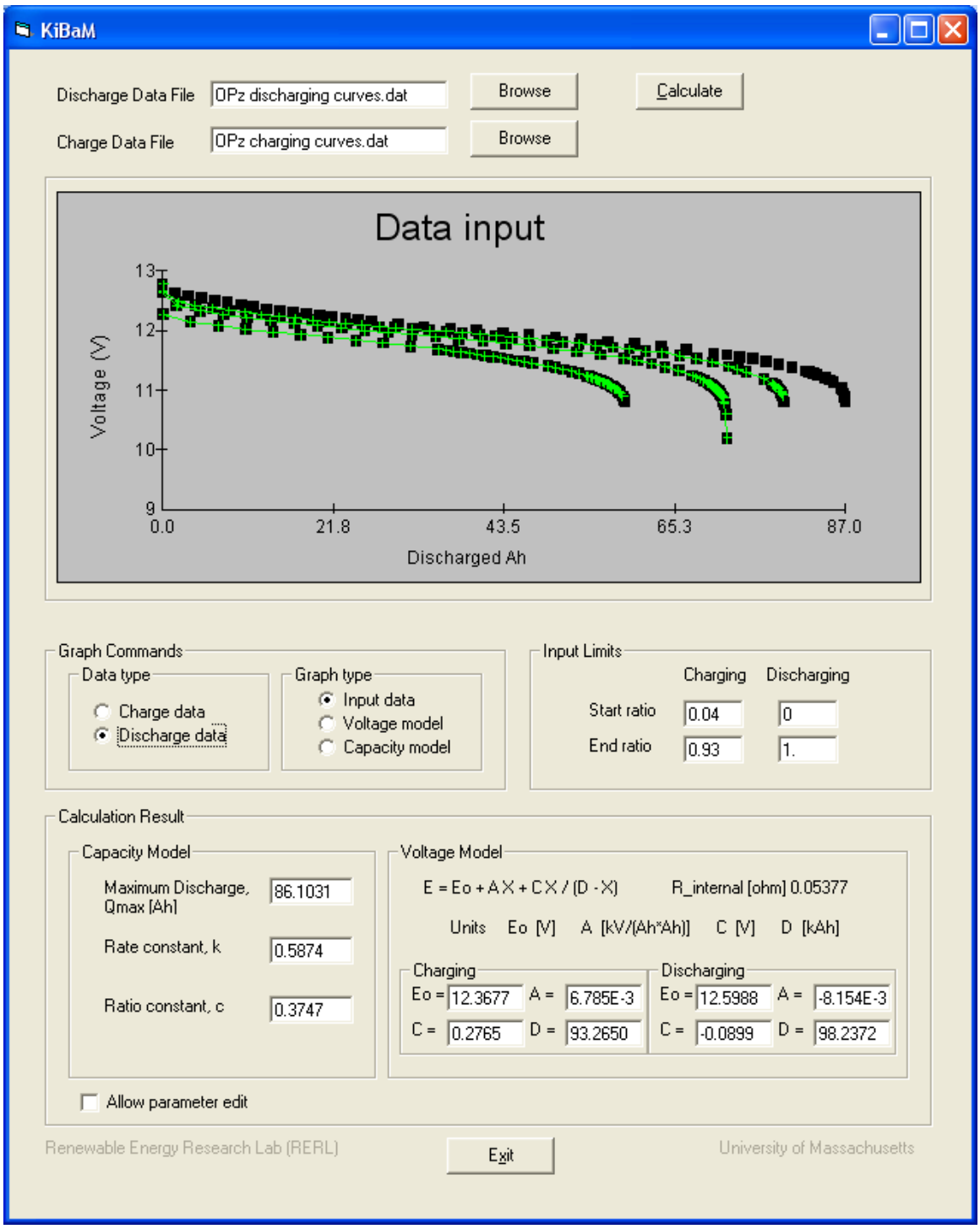

Figure 32 Voltage vs. Charge Removed for OPzS Battery

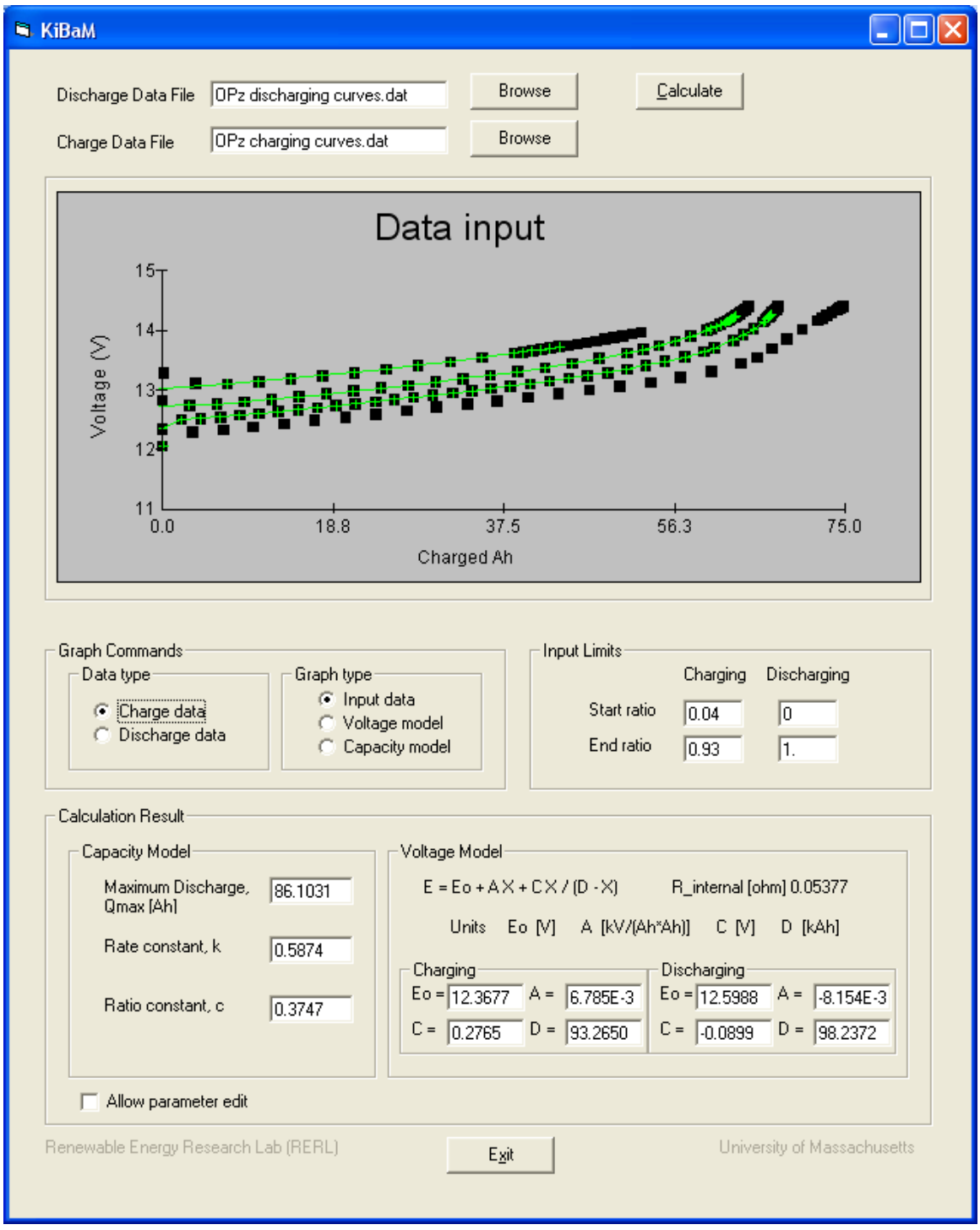

Figure 33 Voltage vs. Charge Added for OPzS Battery

A screen from BatteryParameterFinder.exe illustrating determination of charging voltage constants is shown in Figure 34. The corresponding screen for discharging voltage constants is shown in Figure 35 and the screen for capacity constants is shown in Figure 36.

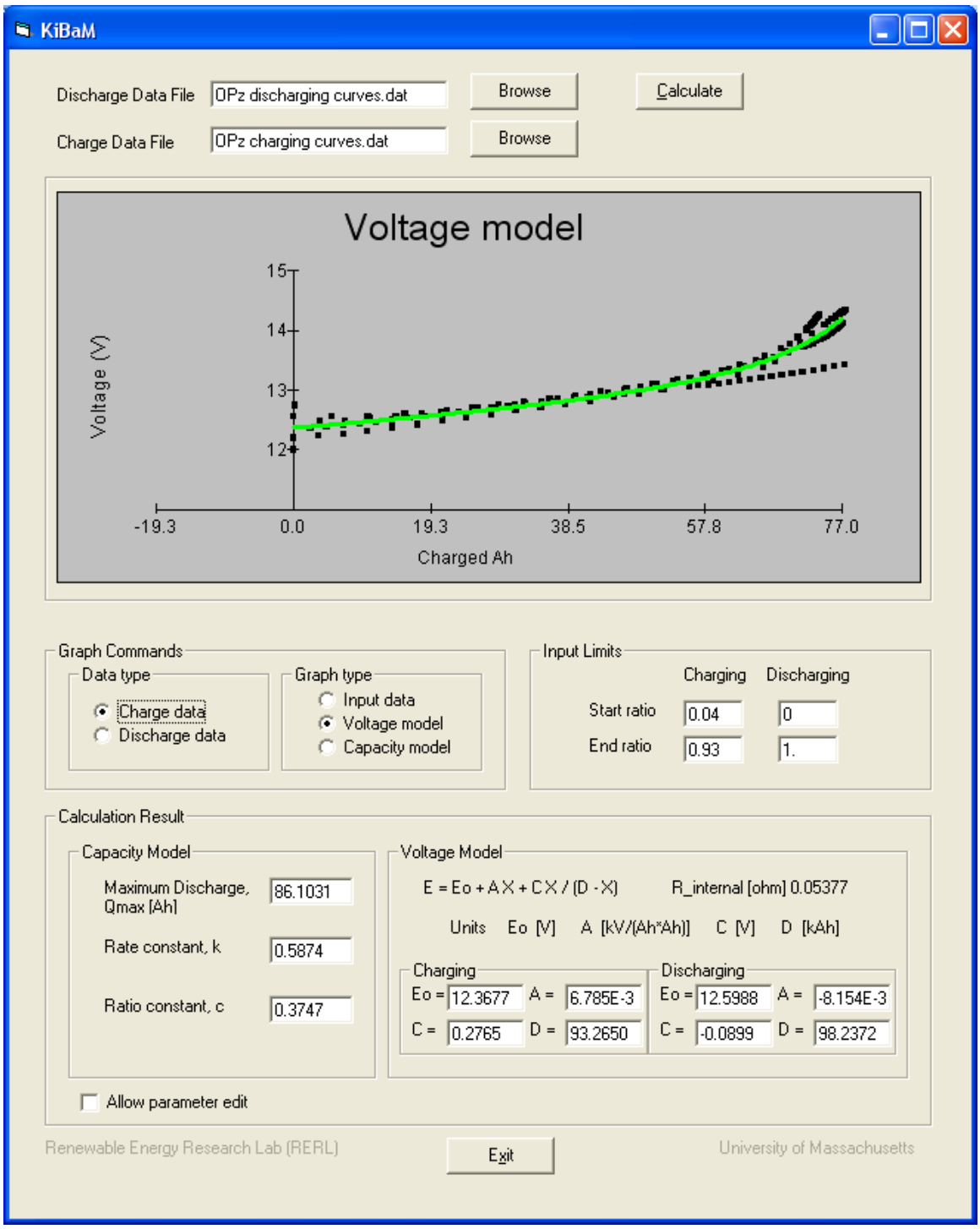

Figure 34 Determination of OPzS Charging Voltage Constants

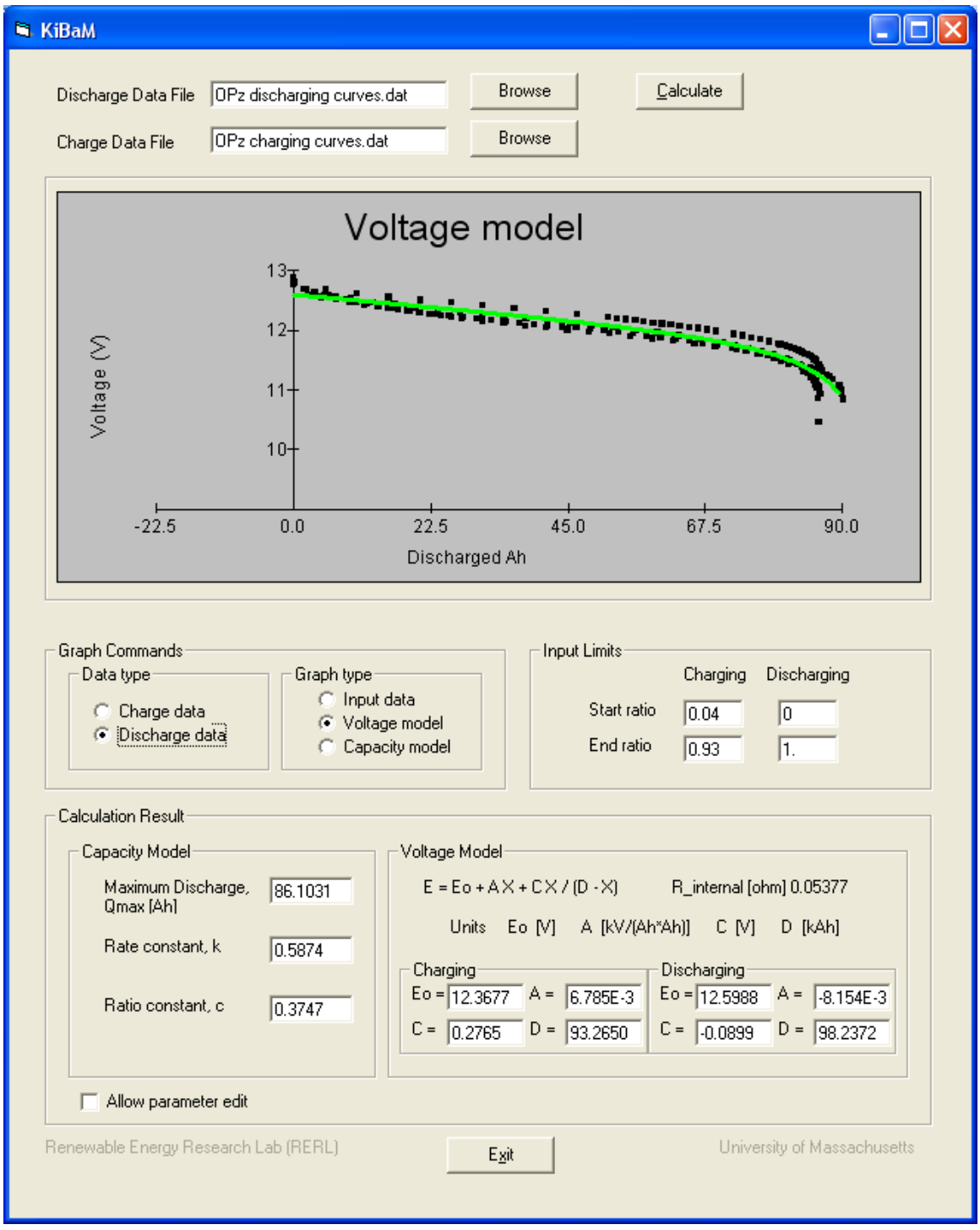

Figure 35 Determination of OPzS Discharging Voltage Constants

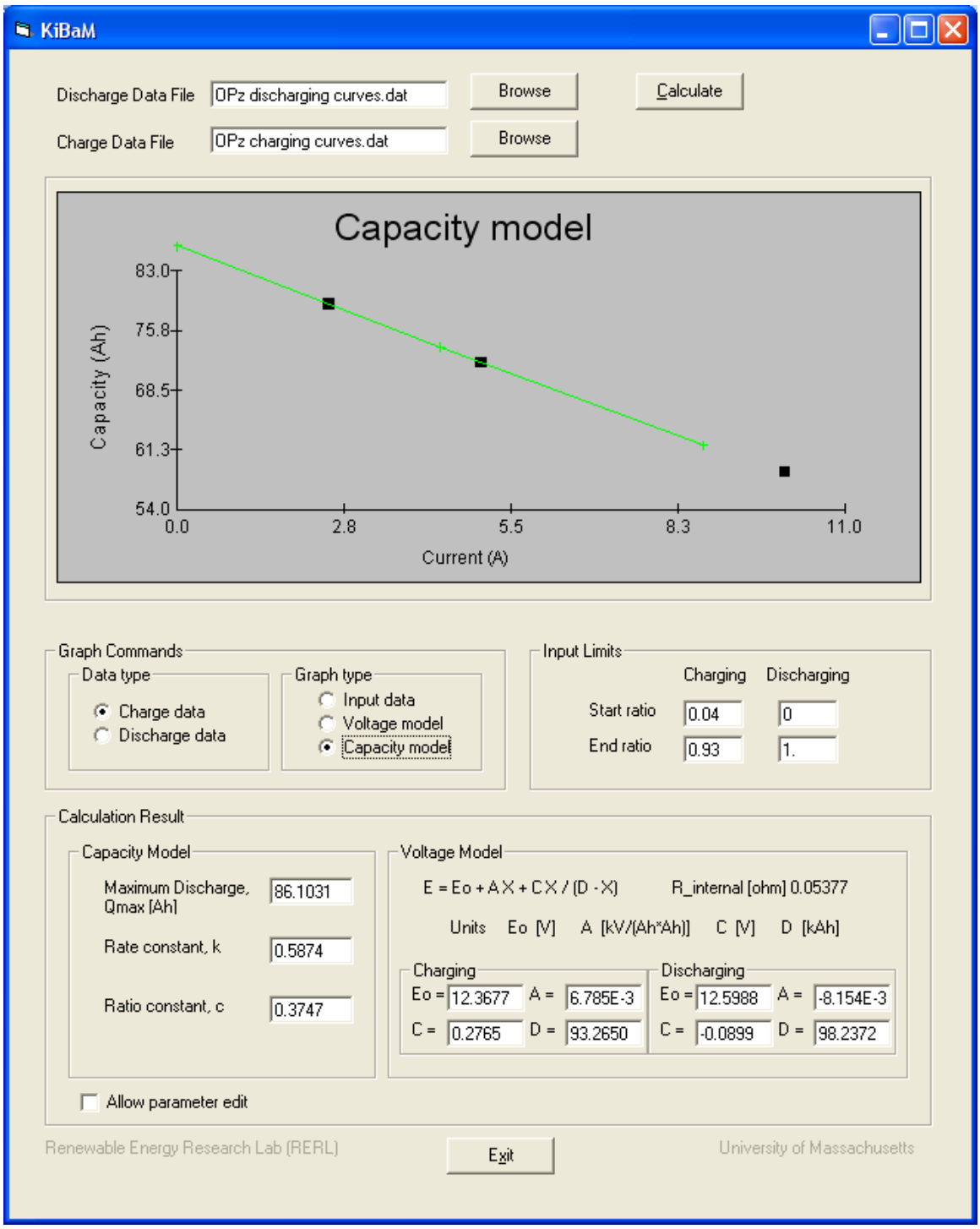

Figure 36 Determination OPzS Capacity Constants

6.3.5.2 Lifetime Constants

The lifetime constants for the OPzS battery were found from data provided by the manufacturer. The 5 constants obtained were: $a_1 = 1380.3$, $a_2 = 6833.5$, $a_3 = 8.750$, $a_4 = 6746.5$, $a_5 = 6.216$.
A curve based on those constants, and the points used to obtain those constants are illustrated in Figure 37.

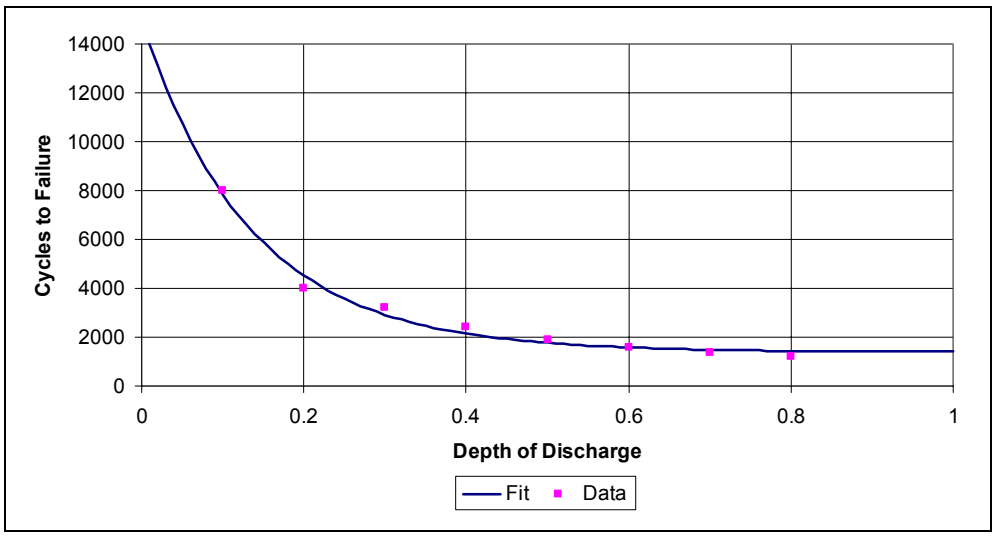

Figure 37 OPzS Battery Life Data and Derived Curve

A screen illustrating input of battery lifetime data for BatteryParameterFinder.exe is shown in Figure 38. A screen illustrating the two curves used in the modified cycle a counter, also as found by BatteryParameterFinder.exe, is shown in Figure 39.

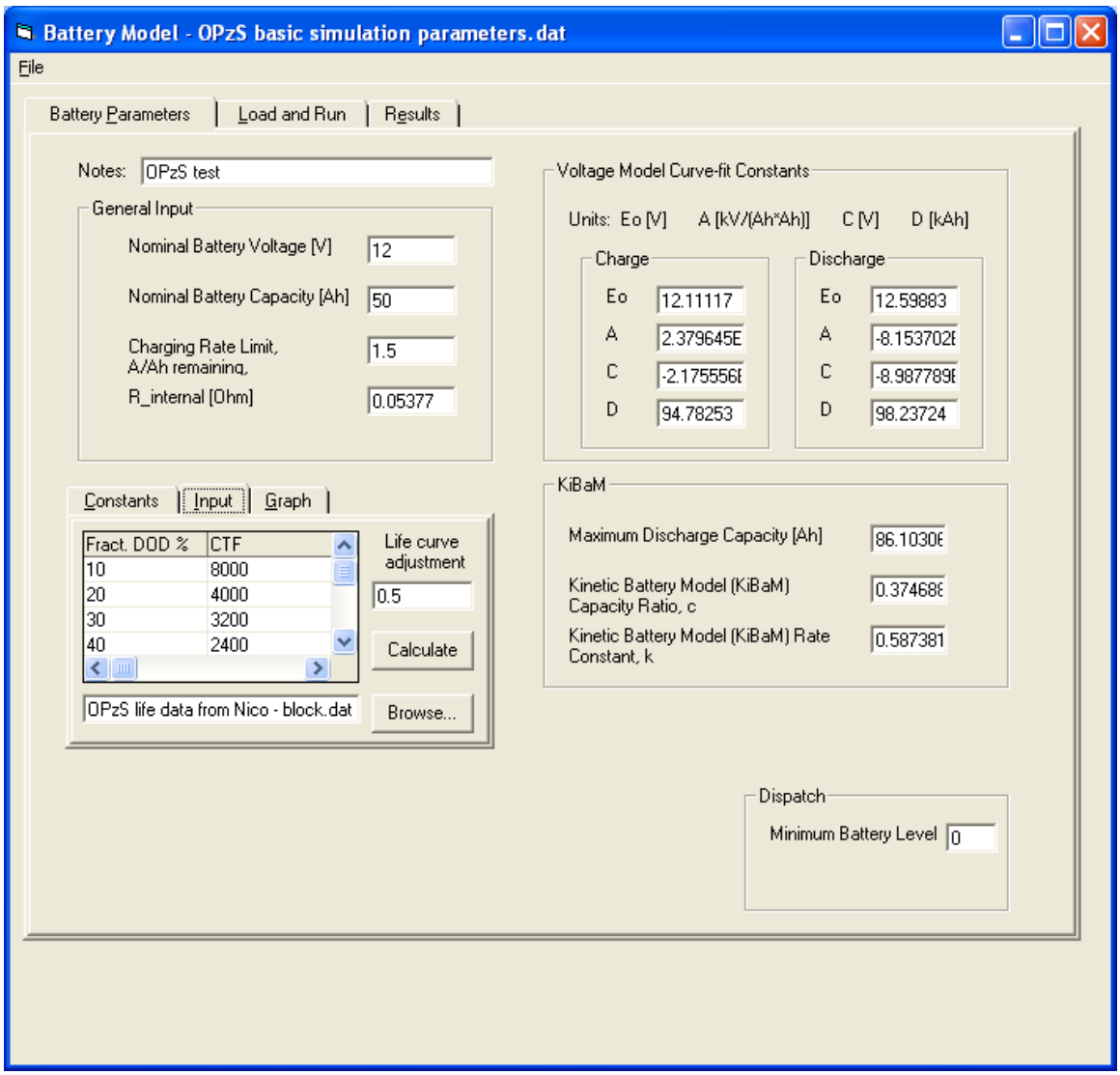

Figure 38 Battery Lifetime Data Input Screen

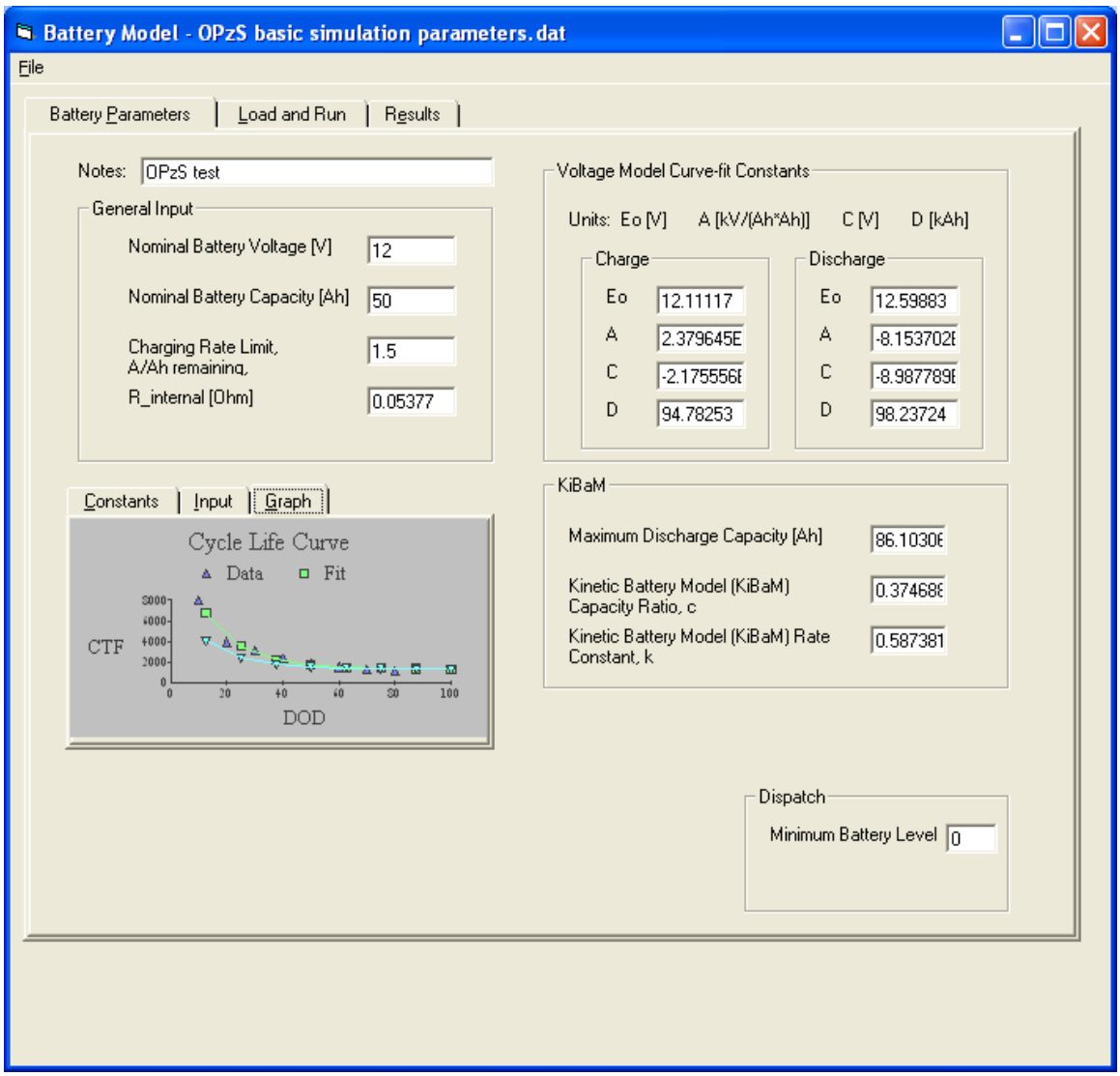

Figure 39 Battery Lifetime Data and Curves

6.4 Simulations

Simulations were carried out to compare the model's predictions with experimental results obtained in the Benchmarking tests. The simulations were designed to mimic the physical tests. Two types of batteries were modelled, the 12 V 2 OGi 50 and the 12 V 1 OPzS 50 using the two renewable system profiles discussed previously. Each battery was loaded with two types of charge/discharge patterns, one representing typical loading in systems with wind turbines and the other representing PV systems. Summary results are described in the next section.

Examples of one set of simulations, focusing on the histograms provided by the modified cycle counter, are shown in the screens in Figure 40 to Figure 42. The screens are from KiBaMBatteryModel.exe. The histograms are in the lower left corner of the screens.

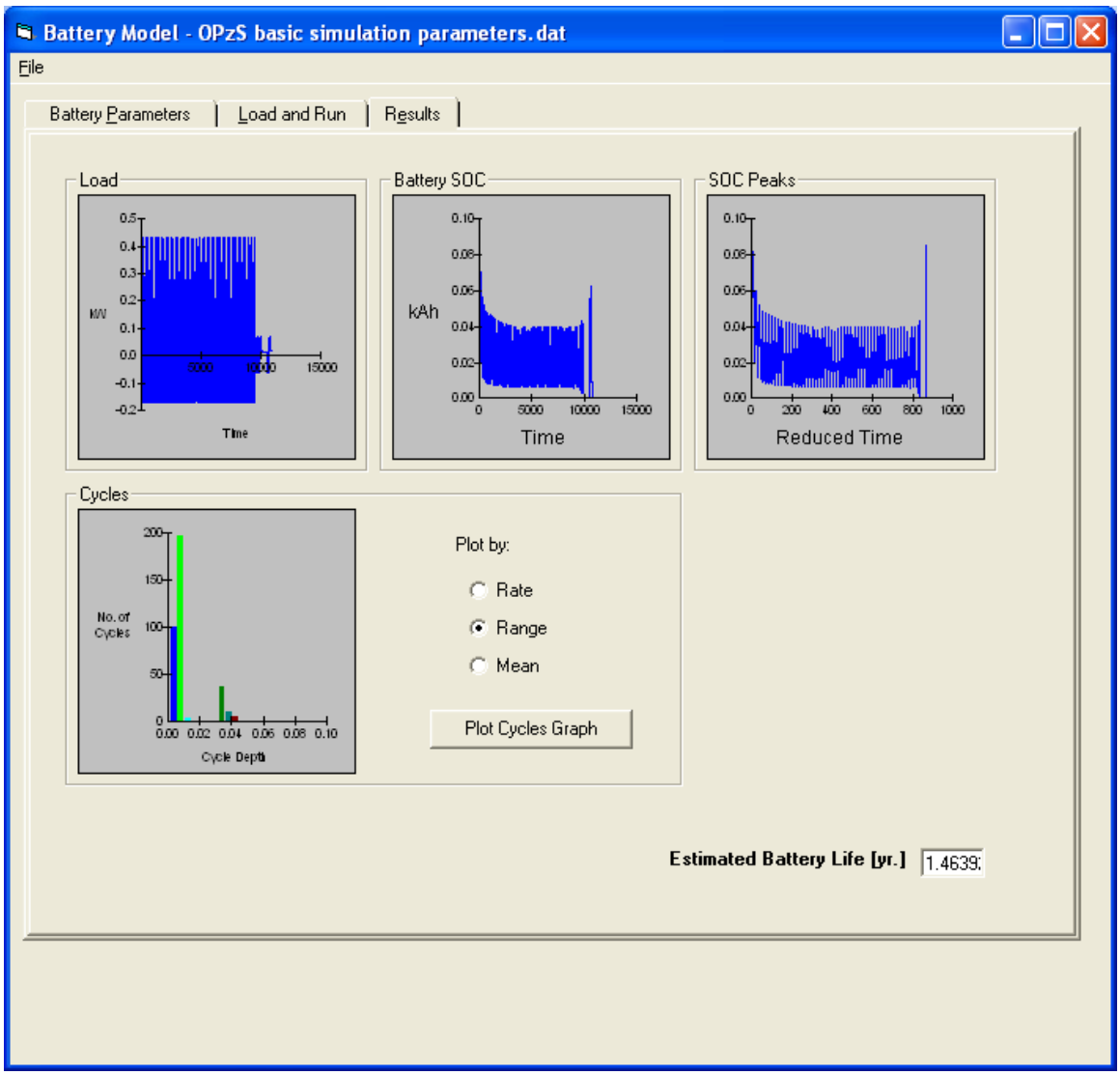

Figure 40 Occurrences of Cycle Depth Range

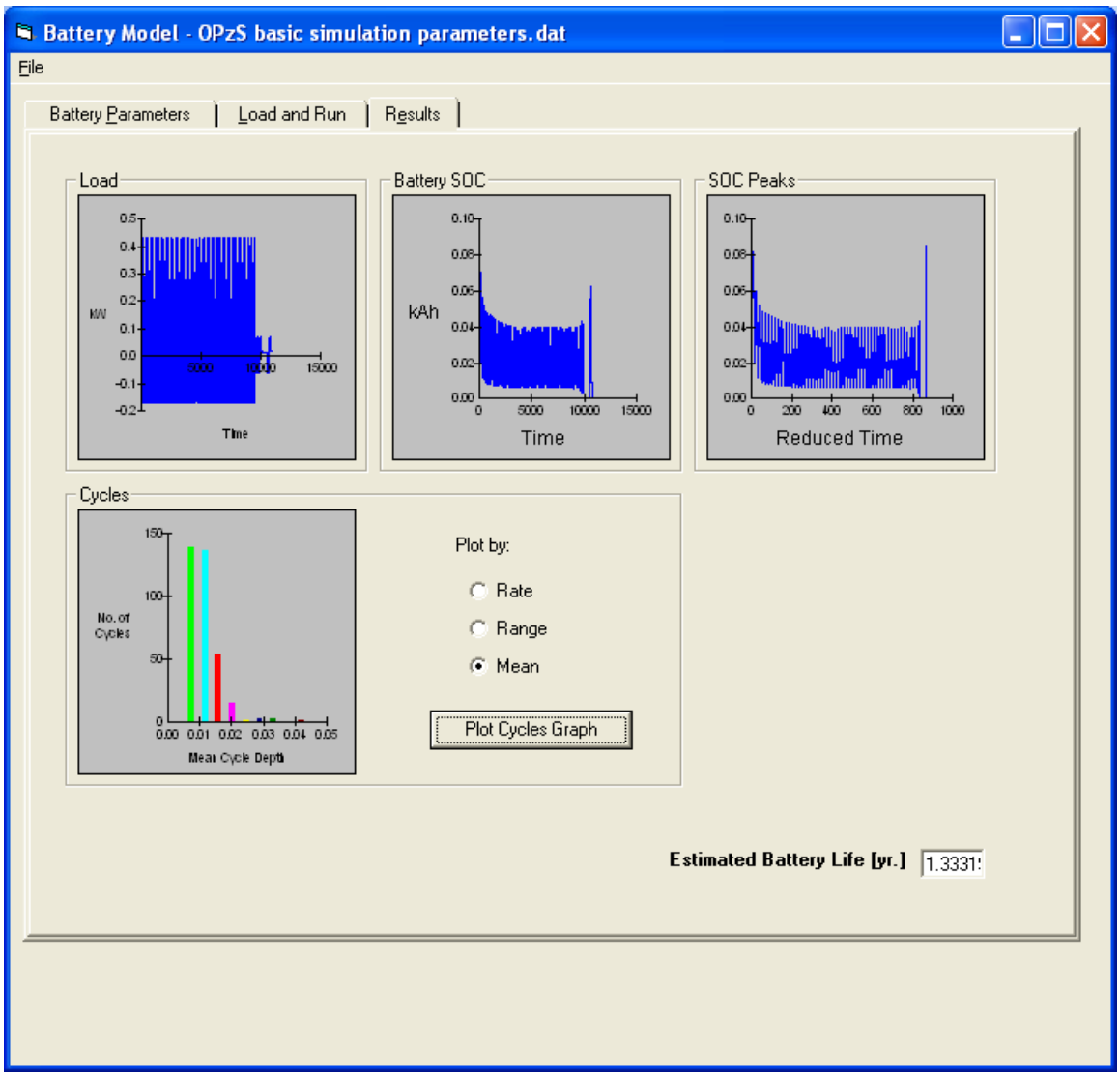

Figure 41 Occurrences of Cycle Mean Values

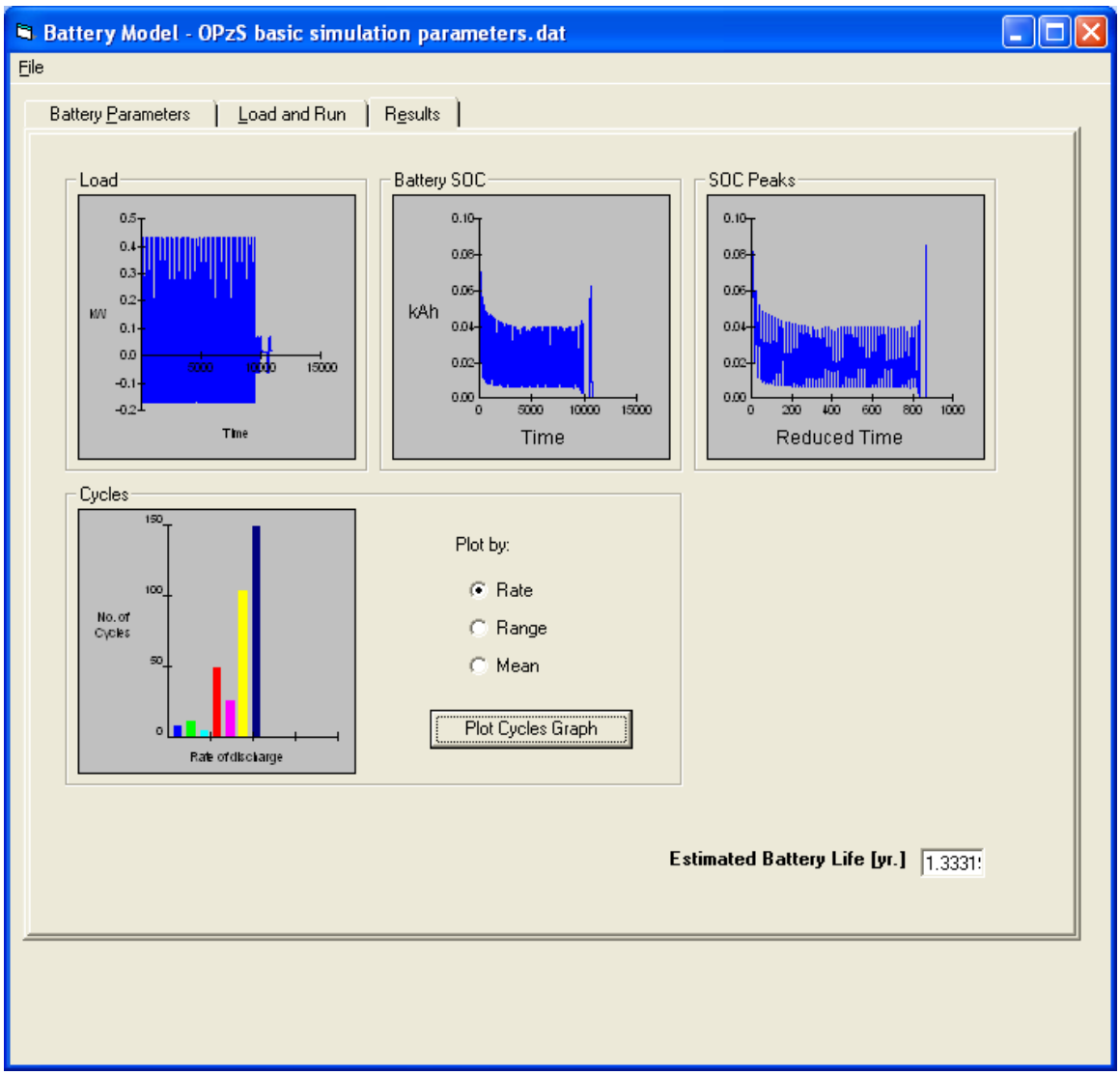

Figure 42 Occurrences of Rate of Discharge

6.5 Comparison with test results for validation before and after model improvements

Table 9 summarizes the experimental results and those of the simulations. The experimental results are shown in the first column and the simulations using the original battery life model in the second column. The third column shows the results of the simulation, using the improved lifetime model. The third column in the first two rows (wind profiles) show the results, assuming the best value of F considered. As expected the predicted lifetime is very close to that observed as a result of fitting the parameter F to the curve. The second two rows illustrate predictions for the PV profiles.

Table 9 Comparison of Experiments and Simulations

	Experiment	Original Simulation	Improved Simulation	Life Curve Adjustment Factor
OGi Wind profile	0.33	0.72	0.33	0.043
OPzS Wind profile	1.0	1.74	1.0	0.11
OGi PV profile	0.66	1.24	0.62	0.043
OPzS PV profile	N/A**	2.89	2.05	0.11

***Data is not available. Tests are still running after 8 months (for OPzS - Nico Peterschmidt's thesis p 50), as of the current date (December 16, 2004)*

The first thing to be noted from the above example is that it was indeed possible to adjust the factor *F* so that it is in the physically expected range and that the simulation model could predict the battery life in the wind profile case. Using the **same** adjustment factor, the simulation model was able to predict a shorter lifetime in the PV profile case than it did without the adjustment factor, as it was hoped it would. The predicted PV life was about half that of the original prediction in the OGi PV profile and about 70% of the original prediction in the case of the OPzS PV profile. The improved prediction for the OGi PV profile is very close to that actually observed. Since the OPzS PV profile experiment had not been concluded as of the time of this writing, no conclusions can be drawn about the accuracy of the model for that case.

The reason for a separate determination of the fitting factor F for OGi and OPzS batteries might be the different design of the batteries. OPzS batteries are more robust against cycling due to the inherent design principle of their tubular plates and thus a higher factor F should be expected and has been determined

7 Discussion of findings

The basic findings regarding the three battery models dealt with in the benchmarking project are that the approaches used each in their own way continue to provide valuable insight in and information about the functioning of batteries in hybrid energy systems. Modifications to the two primary models have enhanced their usability and appear to have improved their ability to predict battery lifetime.

A summary of the overall results is presented in Table 10 below.

Table 10 Summary of the Overall Results

Battery & Profile	Ah Throughput Model (days)	UMass Simulation Lifetime (days)	FhG / Risø Simulation Lifetime (days)	Test Lifetime (days)
OGi1 PV	262	241	660	239
OGi2 Wind	203	120	425	174
OPz1 PV	-	748	830	600+*
Opz3 Wind	266	365	633	400*

** = estimated lifetime(test not yet complete)*

During the model development and verification in the Benchmarking project a number of common battery model related findings and observations were made. The most important issues raised in this context were:

- The results of the model simulations correctly ranked the lifetime of the batteries with respect to the expected outcome of the profiles. That is to say, the wind profile was harsher than the PV and the OPzS can withstand more cycles before failure than the OGi.
- The models use information from the manufacturer's data sheets but the relative performance of the test battery types was not as would be predicted from the data sheet figures. For instance, based on the IEC cyclic data it would be predicted that the life performance of the OGi battery would be slightly shorter than the OPzS battery, however the actual life was much shorter. This may indicate that the damage mechanisms exercised by the test profiles were significantly different from those exercised by the standard manufacturer's tests. Further tests are needed to isolate damage mechanisms so that modelling of these mechanisms can be verified.
- Another explanation for the mismatch in the comparison of the manufacturer's data with the test results may be that the data sheets contain a high margin error, something that has yet to be assessed.
- Since each individual battery usually has a capacity above the manufacturer's nominal rating, the reference capacity for the definition of lifetime requires careful consideration. If the initial capacity is determined for a specific battery then the model may result in a good prediction for that particular battery but it will not be universally applicable because of the spread in initial capacities of any one manufacturer's product. If the battery nominal capacity is used then this may underestimate the life of any one

battery but it will, at least, give a minimum lifetime as the nominal capacity is the figure guaranteed by the manufacturer.

- Whilst the use of a percentage of a reference capacity as the definition of the end of lifetime is simple, it may not be applicable for all remote hybrid power systems. It may be that some performance requirement is better suited for the definition of the end of life.
- The test sequences carried out for parameter fitting for individual batteries and the subsequent parameter fitting procedures themselves were generally satisfactory.
- The results from the battery tests carried out within the Benchmarking project highlighted the variability in performance from battery to battery of the same type from the same manufacturer. This demonstrates the danger of using such statistically small samples to tune the workings of a battery model and reinforces the need to aim for prediction of minimum performance.
- It may turn out to be a problem that the full implementation of a model considering all of the stress factors and damage mechanisms requires data of a type and extent that go beyond what can realistically be expected from battery manufacturers in connection with standard commercial supplies.

8 Status at the end of the project

This section provides a status statement of the model development and validation at the end of the project, including the model-specific requirements for improvements.

8.1 Common Status

The common status for the two primary models is:

- The models have been extracted from being embedded in system simulation models to being separate and stand-alone tools.
- The models have been improved with respect to their representation of battery performance and lifetime, and they have been validated by comparison with lab test measurements undertaken as part of the Benchmarking project [WP4.2 report], [12].
- Test procedures for obtaining battery parameter estimation curves have been established and used successfully on selected project batteries. Furthermore, the procedures for the extraction of the battery parameters have provided the appropriate data for input to the models.
- The availability and application of the models is in accordance with the Consortium Agreement.

Specific conditions for the two models are given below.

8.2 The FhG/Risø Model

The status for the FhG/Risø model at the end of the project :

- The FhG/Risø model is based on a model extracted from an FhG PV system model. The model was further developed and validated in the Benchmarking project in a collaboration between Risø and FhG. The FhG/Risø model is working as a free-standing model in the MATLAB [Version 6.5.1 Release 13] environment.
- The aim of the FhG/Risø model development was to extend its capabilities from RE systems with PV to also include systems with wind power. The main focus in this work was to extend the magnitude of currents and their influence on the damage mechanisms incurred by this particular stress factor.
- The FhG/Risø model development has been validated by comparison with lab test measurements undertaken as part of the Benchmarking project [WP4.2 report], [12].

The most imminent needs for further improvements of the FhG/Risø model are:

- There is a need for more test data to validate mechanisms and assumptions in the model by comparison with both lab tests and full scale systems testing.

- There is a need to validation the model for a wider range of applications by comparison both lab tests and full scale systems testing.
- More stress factors and damage mechanisms from the cross-matrix should be implemented in the model. Extensive battery data sheets should be used to assess the model features to be focused on.
- The use of other test procedures, viz [WP3.2 Report], [15], should be considered to provide input for model parameters and stress factors / damage mechanisms.

It is the intention to include the improved FhG/Risø model in the IPSYS system simulation package being developed at Risø, **Error! Reference source not found.**.

8.3 The UMASS Model

The status for the UMASS model at end of project:

- The UMass battery model, previously only readily accessible in the Hybrid2 simulation model, has been successfully extracted and made more generally useful in a free-standing form.
- A separate code for determining parameters for use in the UMass battery model has been successfully implemented.
- The UMass battery model was able to model rather well the capacity and voltage results of the battery testing undertaken during the Benchmarking project.
- The lifetime portion of the UMass battery model has been successfully expanded to consider cycle means as well as ranges.
- There is in general insufficient test data available to allow the expanded form of the UMass battery life model to be validated and put into general use.
- Promising preliminary results on tracking cycles charge or discharge rates have been obtained, This but more work is required before this capability can could also be put into general use, although some additional programming would be needed and some additional testing and validation would be desirable.

It is apparent that the potential for extending the improvement method has not yet been exhausted. The following are some opportunities for further progress:

- The UMass battery model does not at present consider charge factor. In fact, charge is assumed to be conserved. This may be reasonable for many situations, but is less so when the battery is charged to full capacity. A modification to the UMass model could be made in which a diode to ground is inserted in the circuit, such that current would begin to flow when the terminal voltages reached a certain level. With such a change it would also be possible to include the impact of charge loss on efficiency (in addition to voltage). Or a correction value could be added when the SOC is above 80% and the some of the charging current could be dumped.

- Other possible improvements that would fit into the framework of the model include: (1) standby losses and (2) temperature effects. The rate tracking capability should be more fully explored, and a “time at level” should be added.
- The UMass battery model program output could be extended such that it could report results in a format compatible with the “radar plots” discussed in more detail in other reports prepared under the Benchmarking project. These include: (1) charge factor (if the modification noted above were made), (2) Ampere hour throughput, (3) partial cycling, (4) time at low state of charge, (5) highest discharge rates, and (6) average time between full charge.

It is the intention to implement the improved UMASS model in the Hybrid2, [2], system simulation model developed and made available by UMass and NREL.

8.4 Throughput Model

There are no current plans to improve the throughput model currently implemented in the HOMER software package currently available through NREL. The simplicity of this model allows its use with very limited initial information and although improvements could be made, they would likely require more information about the specific batteries or operating conditions, like temperature, that is not generally available.

9 Recommendations for future work

Although the two lifetime models are at a stage where they may provide quite realistic and useful estimates of lead acid battery performance and lifetime, further development and validation of the two lifetime models should continue. In addition to the issues raised below the items mentioned under section 8 above should also be considered for future work.

The primary recommendation is that more battery lifetime tests need to be carried out to improve the understanding of the damage mechanisms and to further validate the models. Some of these tests should isolate specific damage mechanisms or the impact of different operating conditions, such as the variable impact of cyclic use at different depths of discharge. Sufficient similar tests of specific battery types should be conducted so that any statistical variations between batteries can be accounted for.

The tests should include tests specifically designed to facilitate evaluation and eventual use of each of the improved battery life models. This would include real life system tests with more of the very detailed data sets necessary to represent the battery features and mechanisms.

Increased attention in the model development should be given to the interaction between components and controllers in real life Renewable Energy systems. Ultimately battery lifetime models may develop into complete battery management system models.

Finally, even as the models improve, the data that is needed to assess the life of batteries is becoming more complex at the same time that battery manufacturers are trying to reduce the complexity of the information they provide on specific batteries. More efforts will have to be made to engage battery manufacturers in developing battery life testing algorithms and procedures. As is shown clearly by the mismatch of the IEC cyclic testing, the use of existing testing standards are not overly relevant to their use in isolated power systems.

References

[1] L.H Hansen, P. Lundsager, "*Review of relevant studies of isolated systems*", Risø-R-1109, Roskilde, 2000

[2] J. F. Manwell, A. Rogers, G. Hayman, C. Avelar and J. G. McGowan, *"Hybrid2 Theory Manual"*, Dept. of Mechanical Engineering, University of Massachusetts, Amherst, MA, 01003, USA, 1998, www.ceere.org/rerl/projects/software/hybrid2/Hy2_theory_manual.pdf

[3] HOMER, www.nrel.gov/homer

[4] H. Bindner, O. Gehrke, P. Lundsager, J.C. Hansen, T. Cronin, *"IPSYS – A tool for performance assessment and supervisory controller development of integrated power systems with distributed renewable energy"*, Solar 2004, ANZSES, Perth, Australia, December 2004

[5] V. Svoboda, 2004, *WP3.1 Define performance requirements for energy storage systems in each category.* Center for Solar Energy and Hydrogen Research, Baden-Württemberg, 2004

[6] Lander J.: *"Further Studies on the Anodic Corrosion of Lead in H_2SO_4 Solution*", J. Electrochem. Soc., Vol. 103, No. 1

[7] J. Nickoletatos, S. Tselepis, *"Evaluation of literature search and results of survey about lifetime expectancy of components, in particular the energy storage systems in existing RES applications"*, Benchmark deliverable D1.4, Center for Renewable Energy Sources (CRES), Greece, April 2003

[8] H.-G. Puls, D.U. Sauer, "*Optimisation of stand-alone pv system design and control strategy"*, EuroSun96 , Freiburg, 1996, p813-818

[9] Juergen Schumacher, *"Digitale Simulation regenerativer elektrscher Energiversorgungssystme"*, University of Oldenburg, 1991

[10] O. Bach, H. Colin, D. Desmettre, F. Mattera, "*Testing of batteries used in standalone PV power supply systems"*, Report IEA PVPS T3-11-2002 (2002).

[11] O. Bach, F. Mattera, *"Comparison of different test procedures for lead-acid batteries used in PV systems"* (Preliminary draft, Benchmarking internal communication), June 2003

[12] J. Nickoletatos, S. Tselepis, *"Results and Analysis of Simulated Cycling Tests on Batteries"*, CRES, May 2004

[13] H.-G. Puls, "*Evolutionsstrategien zur Optimierung autonomer Photovoltaik-Systeme",* diploma thesis, Albert-Ludwigs-University of Freiburg, 1997

[14] Matlab, Mathworks, www.mathworks.com

[15] Alan Ruddell, [WP3.2 Report] RAL deliverable 3.2

[16] J. F. Manwell and J. G. McGowan, *"Lead Acid Battery Storage Model for Hybrid Energy Systems*", Solar Energy, 50, No. 5, pp 399-405, 1993.

[17] J. F. Manwell and J. G. McGowan, *"Extension of the Kinetic Battery Model for Wind/Hybrid Power Systems*", Proc. European Wind Energy Conference'94 Thessaloniki, Greece, October, 1994.

[18] Downing, S. D. and Socie, D. F., *"Simple Rainflow Counting Algorithms*", International Journal of Fatigue, January, p 31, 1982.

Mission

To promote an innovative and environmentally sustainable technological development within the areas of energy, industrial technology and bioproduction through research, innovation and advisory services.

Vision

Risø's research **shall extend the boundaries** for the understanding of nature's processes and interactions right down to the molecular nanoscale.

The results obtained shall **set new trends** for the development of sustainable technologies within the fields of energy, industrial technology and biotechnology.

The efforts made **shall benefit** Danish society and lead to the development of new multi-billion industries.